Genome-Wide Identification of Histone Acetyltransferases and Deacetylases in Epiphytic Orchid Plant *Dendrobium Catenatum*

Wei-Wei Jiang
Zhejiang A and F University
Dong-Hai Qu
Zhejiang A and F University
Ji-Li Tian
Zhejiang A and F University
Jin-Ping Si
Zhejiang A and F University
Dong-Hong Chen (chendh212@163.com)
Zhejiang A and F University

Research article

Keywords: HAT, HDAC, histone acetylation, expression profiling, stress response

Posted Date: September 8th, 2020

DOI: https://doi.org/10.21203/rs.3.rs-70072/v1

Abstract

Background: *Dendrobium catenatum* is a kind of precious Traditional Chinese Medicine, and possesses unique developmental programs and epiphytic lifestyle. Histone acetyltransferases (HATs) and histone deacetylases (HDACs) are responsible for maintenance of histone acetylation homeostasis, and they are widely involved in developmental regulation and stress responses via remodeling chromatin structure, but their biological functions in orchid plants remain largely unknown.

Results: Here we identified 8 HAT genes and 14 HDAC genes from *D. catenatum* genome. We carried out phylogenetic construction, gene structure and domain architecture analysis of these *D. catenatum* HAT/HDAC (DcHAT/DcHDAC) proteins using the well-defined homologs from the model plants *Arabidopsis thaliana* and *Oryza sativa* as references. DcHAT proteins can be classified into four families: GNAT family (3 members), MYST family (2), CBP family (2), and TAFII250 family (1), and DcHDAC proteins can be grouped into three families: RPD3/HDA1 family (10), SIR2 family (2), and HD2 family (2), in accordance with previously described classification. Cis-acting element analysis indicated that the promoter regions of DcHAT/DcHDAC genes contain diverse stress-responsive elements. Subcellular localization predictions suggested that DcHAT/DcHDAC proteins might be localized in nucleus or/and cytoplasm. Spatiotemporal expression profiling showed that DcHAT/DcHDAC genes generally exhibit either universal or specific expression pattern in different tissues and organs. Finally, stress response assay suggested drought treatment significantly represses the expression of DcHAG1 and DcHDA14, cold exposure evidently influences the expression of *DcHAG1* and *DcHDT1*, and heat shock has a broad impact on the expression of DcHAT/DcHDAC genes.

Conclusions: In this study, we reveal the identification and expression profiles of DcHATs and DcHDACs in epiphytic orchid plant *D. catenatum*, indicating their roles in the regulation of both long-term developmental programs and short-term stress responses. This study provides a foundation for in-depth functional excavation of HATs/HDACs associated with dynamic histone acetylation levels in orchids.

Background

In eukaryotes, reversible histone acetylation plays a crucial role in dynamic change of chromatin accessibility and regulation of gene expression in response to developmental and environmental cues. In general, histone acetylation and deacetylation are associated with relax chromatin structure for transcriptional activation and compact chromatin for gene repression, respectively [1, 2]. For instance, co-existence of histone acetylation marks H4K16ac and H3K23ac is correlated with high gene expression levels in Arabidopsis [3]. The homeostasis of histone acetylation is antagonistically maintained by histone acetyltransferases (HATs) and histone deacetylases (HDACs), such as HAT member GENERAL CONTROL NON-REPRESSIBLE 5 (GCN5) and HDAC member HDA19 required for H3K36ac homeostasis [4]. The genome-wide identification of HATs and HDACs has been performed in a group of species: *Arabidopsis thaliana* (12 HATs, 18 HDACs) [5], *Oryza sativa* (8 HATs, 18 HDACs) [6, 7], *Vitis vinifera* (7 HATs, 13 HDACs), [8], *Solanum lycopersicum* (32 HATs, 15 HDACs) [9], *Citrus sinensis* (50 HATs, 16 HDACs) [10], *Litchi chinensis* (6 HATs, 11 HDACs) [11], *Malus domestica* (57 HATs, 26 HDACs) [12], *Zea mays* (12 HATs, 16 HDACs) [12], and lower plant *Marchantia polymorpha* (8 HATs, 12 HDACs) [13]. Additionally, There are 11 HDACs in *Populus trichocarpa* [14], 28 HDACs in *Glycine max* [15], 30 HDACs including 15 in each of the A- and D-subgenomes of *Gossypium hirsutum* [16], 9 HATs in either *G. raimondi* or *G. arboretum*, and 18 HATs in *G. hirsutum* [17].

In plant, HATs were divided into four families: TATA-binding protein Associated Factor (TAFII250)/HAF, p300/ cAMP-responsive element Binding Protein (CBP)/HAC, GCN5-related N-terminal AcetylTransferase (GNAT)/HAG and MOZ-Ybf2/Sas3-Sas2-Tip60 (MYST)/HAM [5]. HDACs were classified into three families: Histone Deacetylase 2 (HD2), Silent Information Regulator 2 (SIR2), and Reduced Potassium Dependency 3/Histone DeAcetylase 1 (RPD3/HDA1) that was further divided into three classes: class I (RPD3-like), class II (HDA1-like) and class IV [18]. Both HATs and HDACs associated with dynamic histone acetylation levels have pleiotropic effects on regulation of plant development programs and response to environmental stresses and stimuli. In vegetative phase, histone acetylation regulates the cellular patterning of Arabidopsis root epidermis by relaying positional information, single mutants for HDAC members HDA6, HDA18 and HDA19 and HATs members GCN5 and HAF2 exhibited altered epidermal phenotypes [19, 20]. Arabidopsis GCN5 is implicated in regulating PLETHORA (PLT) gradient-

mediated root stem cell niche maintenance and transit amplifying cell proliferation [21]. AtHAG1/GCN5 is involved in establishment of competence for *de novo* shoot regeneration through acting as an epigenetic switch that renders somatic cells to acquire regeneration potential via catalyzing histone acetylation at key root-meristem gene loci in developing callus [22]. HDA6 and HDA19 function redundantly to repress somatic embryogenesis via suppressing the expression of master embryo regulators; simultaneous knockdown of HDA6/HDA19 causes arrested growth and the formation of embryo-like structures on the true leaves [23]. In reproductive phase, AtGCN5 is required to regulate the floral meristem activity through the WUSCHEL (WUS) / AGAMOUS (AG) pathway, and mutation of AtGCN5 leads to terminal flower, homeotic transformation and ectopic carpel [24]. Arabidopsis HDA9-mediated H3K27 deacetylation is required for Polycomb repressive complex 2 (PRC2) -mediated H3K27me3, leading to *FLC* repression and flowering time regulation [25]. In some crops and vegetables, maize Rpd3/HDA1 member HDA108 is involved in regulation of plant height, shoot and leaf development, male and female inflorescence patterning, and fertility [26]. Cotton GhHDA5 is involved in H3K9 deacetylation and fiber initiation, and knockdown of GhHDA5 suppresses fiber initiation and lint yield [16]. Tomato histones acetylation status affects ethylene-dependent fruit ripening and carotenoid accumulation. Knockdown of *SlHDA1* or *SlHDA3* results in accelerated fruit ripening process along with short shelf life characteristics, but knockdown of *SlHDT3* results in delayed ripening along with prolonged shelf life [27–29]. In terms of environmental stimulus and stress response, histone acetyltransferase TAF1/HAF2 and GCN5 and histone deacetylase HD1 (HDA19) are involved in light regulation of growth and gene expression [30]. HAM1, HAM2 and HAG3 participate in UV-B-induced DNA damage repair and signaling, but HAF1 and HAC1 are only involved in UV-B signaling [31–33]. Populus AREB1 recruits the histone acetyltransferase unit ADA2b-GCN5 to elevate H3K9ac deposition and RNA polymerase II occupancy on drought-responsive genes (*PtrNAC006/007/120*), leading to their activation and increased drought tolerance. Accordingly, disruption of each member of the trimeric AREB1-ADA2b-GCN5 complex causes highly drought sensitivity [34]. Overexpression of a Populus RPD3/HDA1-type gene 84KHDA903 in tobacco enhanced drought tolerance [35]. In fact, Lys acetylation-mediated posttranslational regulation occur not only on histones, but also on nonhistone proteins. SRT2 can target the ATP synthase and the ATP/ADP carriers, fine-tuning mitochondrial energy metabolism [36]. HDA6 can deacetylate the K189 residue of BIN2 to inhibit its kinase activity and increase brassinosteroid signaling in Arabidopsis [37].

Tiepi-Shihu (*Dendrobium catenatum*, or *D.officinale*, or *D. candidum*) is a rare traditional Chinese medicinal plant in Orchidaceae [38], for their traditional properties of nourishing the kidney, moisturizing the lung, benefiting the stomach, promoting the production of body fluids and clearing heat [39]. The earliest records of *Dendrobium* utilization date back to"*Shen Nong's Herbal Classic*"(□□□□□) written nearly 2,300 years ago during the Eastern Han Dynasty. Especially,*Dendrobium* was listed as the head of the nine Chinese fairy grasses in "*Collected Taoist Scriptures*"(□□) during the Tang Dynasty. At present, *D. officinale* Kimura et Migo is individually listed in *Pharmacopoeia of the People's Republic of China* (2015 Edition) for rich polysaccharides, whereas *D. nobile* Lindl., *D. chrysotoxum* Lindl. and *D. fimbriatum* Hook. are uniformly classified in the item of *Dendrobium* with dendrobine, erianin and dendrophenol as the active ingredients, respectively [40]. Modern pharmacological study suggested that *D. catenatum* possesses hepatoprotective, anticancer, hypoglycemic, antifatigue, antioxidant, anticonstipation, hypoglycemic, gastric ulcer protective, and antihypertensive effects, immunoenhancement, and so on [41].

The biological functions of HATs and HDACs in *D. catenatum* remain unknown, so a genome-wide analysis of HAT and HDAC superfamilies was performed to gain insight into their potential roles. In this study, we identified 8 HAT genes and 14 HDAC genes throughout the genome of *D. catenatum*. Evolutionary relationships of DcHATs and DcHDACs were assessed through phylogenetic reconstruction, gene structure and domain organization. Promoter cis-acting element and protein subcellular localization were investigated using online software. Gene expression profiling in different tissues or organs as well as stress responses were determined via RNA-seq data and quantitative RT-PCR. Together, our results shed light on the involvement of HATs and HDACs in growth and development as well as environmental fitness of *D. catenatum*, and contribute to further investigate the evolution and function of histone acetylation in orchid medical plants.

Results

Identification of HAT and HDAC genes in *D. catenatum*

HATs and HDACs are responsible for catalyzing the deposition and removal of acetyl groups from histones, respectively. Both classes of enzymes finetune genome-wide histone acetylation status, leading to modification of chromatin structure, fluctuation of gene expression and reprogramming of developmental progresses. To obtain all the HAT and HDAC homologs in *D. catenatum*, the well-examined respective HAT and HDAC proteins in both Arabidopsis and rice were used as queries to BLASTp against *D. catenatum* genome; then the hits were further confirmed through reciprocal BLAST. Ultimately, 8 HAT genes and 14 HDAC genes were obtained in *D. catenatum* (**Table 1** and **Additional file 1**), and they were named by reference to the corresponding Arabidopsis homologs with the prefix"Dc"for distinguishing. Of the 8 DcHATs, 3 members belong to the GNAT family, 2 belong to the MYST family, 2 belongs to the CBP family and 1 belongs to the TAFII250 family. Of the 14 DcHDACs, 10 belong to the RPD3/HDA1 family, 2 belong to the SIR2 family and 2 belong to the HD2 family.

HAT: p300/CBP/HAC family

To determine the evolutionary relationship of DcHATs with those from rice, and Arabidopsis, total protein sequences from these organisms were used to construct a neighbour-joining phylogenetic tree (Fig. 1). We observed one subgroup related to CBP, TAFII250 and MYST, and three subgroups for GNAT. Eight DcHATs can be divided into four families, CBP (DcHAC1a/1b), GNAT (DcHAG1/2/3), TAFII250 (DcHAF1), and MYST (DcHAM1/2). HAT/HDAC members in *D. catenatum* usually have extremely longer genomic sequences than those in Arabidopsis and rice (Fig. 2), largely owing to existence of overlength introns.

The CBP family contains 5 members in Arabidopsis, 3 in rice and 2 in *D. catenatum* (Fig. 1). HAC-like proteins are usually characteristic of several successive domain combinations: an N-terminal ZnF-TAZ domain, a PHD-finger domain, a CBP-type HAT domain, a ZnF-ZZ domain and a C-terminal ZnF-TAZ domain, except AtHAC2 and OsHAC5 lacking the N-terminal ZnF-TAZ domain. Phylogenetic analysis (Fig. 1) revealed that DcHAC1a/1b paralog pairs were grouped together with AtHAC1/12 and OsHAC1a/1b pairs, consistently, DcHAC1a and DcHAC1b have 74.1% protein sequence identity, both display 51.6% and 50.5% identity with AtHAC1, respectively. No counterparts in *D. catenatum* were classified into AtHAC4/5, OsHAC5 or AtHAC2 branches, indicating CBP family in *D. catenatum* might have experienced less gene duplication events during evolution. In Arabidopsis, AtHAC1 participates in pleiotropic developmental programs, and its mutation causes delayed flowering, decreased primary root length, and poor fertility [42]. AtHAC5 and AtHAC12 have redundant functions with AtHAC1 in regulate flowering time by repressing the expression of a major floral repressor *FLC* [43]. AtHAC1/5 are required for salicylic acid (SA)-triggered immunity and PR induction. AtHAC1/5 together with the master immune regulator NPR1 are recruited to PR chromatin through NPR1 interacting with transcription factor TGA upon SA signal, resulting in the formation of HAC-NPR1-TGA complex that activates PR transcription by histone acetylation-mediated epigenetic reprogramming [44]. So, DcHAC1a/1b might undertake most of HAC roles in development regulation and stress response of *D. catenatum*.

HAT: GNAT/HAG family

HAG family was divided into three distinct clades (HAG1/GCN5, HAG2 and HAG3/ELP3), each of which contains a single member in examined species. All HAG family proteins possess a landmark GNAT-type HAT domain (Acetyltransf_1, PF00583), moreover, each clade has additional distinct domains, such as HAG1/GCN5 with a C-terminal bromodomain, HAG2 with Hat1_N domain (PF10394) and HAG3 with a central Elp3 domain (IPR006638). Bromodomain found in many chromatin-associated proteins can interact specifically with acetylated lysine and mediate the interaction between histone acetyltransferases and histone proteins [45]. In HAG1 clade, Arabidopsis AtGCN5/HAG1 is a major HAT and usually acts as the catalytic subunit of several multicomponent HAT complexes that acetylate lysine residues of histone H3 [46]. AtGCN5/HAG1 plays an essential role in diverse plant development processes, such as meristem activity, cell differentiation, plant architecture, root, leaf and floral organogenesis, and *de novo* shoot regeneration [21, 22, 24, 46, 47]. AtGCN5/HAG1 is also involved in nutrient balance and fatty acid metabolism. AtGCN5 contributes to iron homeostasis by directly affecting the H3K9 and H3K14 acetylation level of the citrate efflux protein FRD3. Mutation of AtGCN5 impairs iron translocation from the root to the shoot [48]. AtGCN5 modulates fatty acid biosynthesis by affecting the H3K9/14 acetylation levels of FAD3; loss of AtGCN5 causes decreased ratio of α-linolenic acid to linoleic acid in seed oil [49]. AtGCN5 regulates stem cuticular wax biosynthesis by modulating the H3K9/14 acetylation of CER3; AtGCN5 disruption impairs cuticular wax accumulation [50]. In addition,

AtGCN5/HAG1 is involved in response to environmental stresses. AtGCN5 is required for thermotolerance and salt tolerance through H3K9/14 acetylation and activation of the key stress-responsive genes [51, 52]. DcHAG1 displays same domain organization with other plant GCN5 proteins, shares 62.5% and 63.4% sequence identity with AtHAG1/GCN5 and OsHAG1, respectively. But the GNAT-type HAT domain of DcHAG1 is 88.3% sequence identical to that of AtHAG1/GCN5. Considering the significance of HAG1 clade, it is requisite to investigate the regulatory function of DcHAG1 in *D. catenatum*. In HAG3 clade, Arabidopsis HAG3 participates in UV-B-induced DNA damage repair and signaling. Knockdown of *HAG3* leads to reduction of DNA damage and growth inhibition by UV-B [31]. DcHAG3 has 88.4% and 90.4% sequence identity with AtHAG3 and OsHAG3, respectively, indicating DcHAG3 might have similar role in UV-proof.

HAT: TAFII250/HAF family

Dendrobium genome contains a single TAFII250 homolog DcHAF1, like rice with one homolog OsHAF1, but different from Arabidopsis with a twin copy AtHAF1/2 (Fig. 1). DcHAF1 gene consists of 20 exons, OsHAF1 contains 22 exons and AtHAF1/2 contain 21/17, respectively. However, the genomic sequence of DcHAF1 is nearly 90 kb long due to extremely large introns, much longer than that of OsHAF1 (14 kb) and AtHAF1/2 (10/8 kb). HAF1 encoding proteins in the examined species are about 2000 aa long, and DcHAF1 shares 46.7% and 53.3% amino acid sequence identity with AtHAF1 and OsHAF1, respectively. HAF proteins are usually characterized by coexistence of an N-terminal TBP-binding domain, a DUF3591 domain, a C2HC-ZnF domain, and a C-terminal bromodomain. DUF3591 domain is a unique HAF-type HAT domain, which encompasses a N-terminal UBQ motif, influencing protein function in a nonproteolytic manner [53]. Bromodomain can specifically recognize acetyl-lysine (Kac) and is functionally linked to the HAT activity of co-activators in regulating gene transcription [45]. Phylogenetic analysis revealed DcHAF1 clustered together with OsHAF1 to form monocot branch with high bootstrap value, whereas AtHAF1/2 cluster together to represent dicot branch, suggesting a duplication event might occur near the origin of dicots. In Arabidopsis, HAF2 (TAF1) gene is involved in integrating light signals and activating light-responsive gene transcription through histone acetylation; *haf2* mutant displays reduced chlorophyll accumulation, pale cotyledon and yellowish young leaf [54]. HAF2 facilitates H3 acetylation deposition at the promoters of the core clock genes *PRR5* and *LUX* to contribute to stable maintenance of circadian oscillation [55]. It is intriguing to unveil the biological mechanism underlying the divergence of HAF gene copy number between dicot and monocot during evolution.

HAT: MYST/HAM family

D. catenatum genome has two MYST-like genes, DcHAM1/2, but so far both only have partial sequences available (Fig. 1). Based on known full-length MYST sequences in other species, MYST family members usually share the conserved domain combinations: an N-terminal chromodomain, a central C2H2-ZnF domain and a C-terminal MYST-type HAT domain MOZ-SOS. Chromodomain is a methyl-specific histone binding module [56], indicating that MYST-catalyzed histone acetylation might coordinate with histone methylation to perform the functions. In Arabidopsis, HAM1 and HAM2 act redundantly to control female and male gametophyte development as well as flowering time. Knockout of HAM1 and HAM2 resulted in lethality; in *ham* sesquimutants *ham1/+*; *ham2/ham2* and *ham1/ham1;ham2/+*, half of the ovules aborted due to an arrest of mitotic cell cycle at one-nucleate stage of megagametogenesis [57]. On the other hand, HAM1 and HAM2 regulate flowering time by deposition of histone H4 lysine 5 acetylation (H4K5ac) within *FLC* and *MAF3/4* chromatins; knockdown of *HAM1/2* by amiRNA or T-DNA insertion results in early flowering and reduced fertility, whereas overexpression of HAM1 caused late flowering [58].

HDAC: PRD3/HDA1 family

To determine the evolutionary relationship of DcHDACs with those from rice, and Arabidopsis, total protein sequences from these organisms were used to construct a neighbour-joining phylogenetic tree (Fig. 3). HDACs were grouped into three families, SIR2, HD2, and RPD3/HDA1, which is further divided into Class-I, II, and IV. For the members in each family or clade, the closer the genetic relationship, the more similar the gene structure (Fig. 4). All Dendrobium RPD3/HDA1 members contain the conserved histone deacetylase domain (Hist_deacetyl) (Fig. 3), but their length varies from 356 aa to 685 aa, except DcHDA2b and DcHDA5b with partial sequences. In addition, DcHDA9 has another transmembrane domain at N-terminus, whereas

DcHDA15 possesses another ZnF_RBZ domain, which was found in a nucleoporin protein RanBP2 located on the cytoplasmic side of the nuclear pore complex functioning in nuclear protein import [59].

Class-I of RPD3/HDA1 family possesses 10 members in *D. catenatum*, 12 in Arabidopsis, and 14 in rice; and they can be divided into four subclasses: I-1 (HDA19), I-2 (HDA6/7), I-3 (HDA9/10/17), and rice-specific I-4 (HDA701/709). Subclass I-1 compresses a single member each in *D. catenatum* and Arabidopsis, and 3 homologs in rice. In Arabidopsis, down-regulation of *HDA19* (*AtHD1*) leads to pleiotropic defects including early senescence, serrated leaves, aerial rosettes formation, delayed flowering, and defects in floral organ identity [60, 61]. Deplete of *HDA19* results in markable tolerance to abiotic stresses including salinity, drought, and heat [62, 63]. In rice, knockdown of *HDA703* (*OsHDAC3*) reduces rice peduncle elongation and fertility, knockdown of *HDA710* (*OsHDAC2*) affects vegetative growth, and down-regulation of *HDT702* (*OsHDAC1*) causes the production of narrowed leaves and stems [7]. overexpression of *HDA702* enhances growth rate, alters plant architecture [64], and increases root growth through deacetylating *OsNAC6* locus [65]. HDA702 implicates in formation of IDS1-TPR1-HDA1 transcriptional repression complex, contributing to negative regulation of salt tolerance [66]. These data suggest that HDA702/703/710 in rice may have divergent developmental functions compared with closely related homologs in Arabidopsis. DcHDA19 has 77.6% and 77.4% sequence identity with AtHDA19 and HDA702, respectively. It is interesting to explore whether the function of DcHDA19 is more near to AtHDA19 or HDA702. Subclass I-2 harbors a single copy each in *D. catenatum* (DcHDA6) and rice (HDA705), and two homologs in Arabidopsis (AtHDA6/7). Arabidopsis HDA6 is involved in leaf development [67], cellular patterning of root epidermis [68], flowering time [69], repression of somatic embryogenesis [23], circadian rhythms [55], and light intensity adaption [70]. AtHDA6 is also required for repressing pathogen defense response; loss of HDA6 resulted in enhanced resistance to hemibiotrophic bacterial pathogen Pst DC3000 and constitutively activated expression of pathogen-responsive genes [71]. AtHDA7 is crucial for female gametophyte development and embryogenesis, and silencing of AtHDA7 causes reduced seed set [72]. In rice, overexpression of *HDA705* in rice decreases the resistance to ABA and salt stress during seed germination, but enhances the resistance to osmotic stress during the seedling stage [73]. DcHDA6 has 67.2% and 66.6% sequence identity with AtHDA6 and HDA705, respectively, but only 49.9% with AtHDA7, indicating the function of DcHDA6 is more near to AtHDA6 than AtHDA7. Subclass I-3 consists of a single member each in *D. catenatum* and rice, and 3 members in Arabidopsis. Arabidopsis HDA9 is involved in preventing precocious flowering under short day [74, 75], suppressing seed germination [76], and promoting the onset of leaf senescence [77]. Moreover, the *hda9* mutant is insensitive to salt and polyethylene glycol treatments [78]. DcHDA9 has 78.5% sequence identity with AtHDA9, indicating there might be functional similarity to a large extent.

Class-II of RPD3/HDA1 family contains 5 members each in *D. catenatum*, Arabidopsis and rice; and they can be divided into four subclasses: II-1 (HDA8), II-2 (HDA14), II-3 (HDA15), and II-4 (HDA5). Among them, subclass II-3 possesses a single member in *D. catenatum*, Arabidopsis, and rice. DcHDA15 contains an additional ZnF_RBZ domain (SMART, SM00547), and shares the sequence identity of 53.2% and 55% with AtHDA15 and OsHDA704, respectively. DcHDA15 gene, like rice HDA714, consists of 16 exons, but is around 112 kb in length, far larger than HDA714 (~ 20 kb). In Arabidopsis, HDA15 is a negative component of light-regulated seed germination. PHYTOCHROME INTERACTING FACTOR3 (PIF3) recruits HDA15 to repress chlorophyll biosynthesis and photosynthesis gene expression in etiolated seedlings [79]. HDA15-PIF1 acts as a key repression module directing the transcription network of seed germination [80]. NF-YC1/3/4/9 transcriptional co-repressors interact with HDA15 to inhibit hypocotyl elongation in the light partially via histone deacetylation [81]. Collected date suggested that DcHDA15 might have a role in photomorphogenesis and skotomorphogenesis. Subclass II-4 has a pair of paralogs in *D. catenatum* (DcHDA5a/b) or Arabidopsis (HDA5/18), and one member in rice (HDA713). DcHDA5a has the sequence identity of 53.8% and 59.4% with AtHDA5 and OsHDA713, respectively. In Arabidopsis, HDA5 regulates flowering time through targeting the chromatin of flowering repressor genes *FLC* and *MAF1* as well as interacting with FVE, FLD and HDA6 to form a complex. The *hda5* mutant is late-flowering due to up-regulated expression of *FLC* and *MAF1* associated with increased deposition of activation markers, histone H3 acetylation and H3K4 trimethylation (H3K4me3) [82]. HDA18-mediated histone acetylation affects cellular patterning in root epidermis, and loss or overexpression of *HDA8* lead to cells at the N position having H fate [83].

Class-IV of RPD3/HDA1 family contains 2 copies in *D. catenatum*, but only a single member in Arabidopsis and rice, respectively. DcHDA2a displays protein sequence identity of 61.7% and 71.1% with AtHDA2 and OsHDA706, respectively. No related function was reported so far.

HDAC: HD2 family

HD2 family is specific to plant, and firstly appeared in Streptophyta green algae Charophyta, but not in Chlorophyta [84]. Here we identified two HD2 homologs in *D. catenatum* (DcHDT1/2), compared with 2 members in rice (HDT701/702) and 4 members in Arabidopsis (AtHD2A-D). HD2-like genes usually compress 7 ~ 9 exons and about 1 kb in length (Fig. 4) but they have significant sequence divergence during evolution. For instance, there are only 50.6% protein sequence identity between DcHDT1 and DcHDT2, which both also share 17.9% and 45.9% sequence identity with OsHDT701, 24.5% and 7.2% with OsHDT702, respectively. DcHDT1/2 are characterized of the conserved C2H2-type zinc finger domain at C-terminus, but this domain is loss in Arabidopsis AtHD2A/2C and rice HDT702. HD2 proteins lacking zinc finger domain (Gr2 HD2s) evolved from those containing zinc finger domain (Gr1 HD2s) during angiosperm diversification, and Gr2 HD2s might fulfill complementary functions with the corresponding Gr1 HD2s [84]. In Arabidopsis, HD2 histone deacetylases have been demonstrated to participate in repressing gene expression [85]. HDT1 (HD2A) and HDT2 (HD2B) paralogs are involved in regulating root meristem maintenance partially through fine-tuning gibberellin metabolism via deacetylation and repression of *GA2ox2* [86]. HD2B was identified as a distinguished factor associated with seed dormancy by genome-wide association mapping of 113 wild-type accessions with natural variation; inactivation of HD2B contributes to maintenance of seed dormancy in dormant accessions [87]. In addition, HD2 family is involved in the response to biotic and abiotic stresses. HD2B is implicated in plant innate immune defense in the form of MPK3-HD2B regulatory module [88]. Loss of HD2C results in hypersensitivity to ABA, NaCl and salt stress [89]. Overexpression of *HDT701* in rice reduces resistance to ABA, salt and osmotic stress during seed germination, but enhances resistance to salt and osmotic stress during the seedling stage [90]. Further work is required to exploit why Gr2 HD2s is loss in *D. catenatum* during evolution.

HDAC: SIR2 family

SIR2 family contains 2 members in *D. catenatum*, Arabidopsis, and rice, respectively. All these proteins possess a single copy of SIR2-type HDAC domain, whose catalytic activity requires NAD as a cofactor [91]. SIR2 family was divided into two clades, SRT1 clade including DcSRT1/AtSRT1/OsSRT701 and SRT2 clade including DcSRT2/AtSRT2/OsSRT702, indicating SRT1/2 diverged before the split of dicot and monocot. Consistently, the members in SRT1 or SRT2 branch have similar exon-intron gene structure architecture, respectively. Protein alignment showed DcSRT1 shares sequence identity of 60.3% and 62% to AtSRT1 and OsSRT701, respectively. DcSRT2 shares 66.6% and 61.4% sequence identity with AtSRT2 and OsSRT702, respectively. In Arabidopsis, SRT2 but not SRT1 is localized at the inner mitochondrial membrane and interacts with some protein complexes, mainly involved in energy metabolism and metabolite transport. Mutation of *SRT2* results in no growth phenotype but rather a metabolic disorder with altered levels in sugars, amino acids, and ADP contents [36]. AtSRT1 negatively regulates plant tolerance to stress and glycolysis but stimulates mitochondrial respiration through both epigenetic regulation and modulation of AtMBP-1 transcriptional activity [92]. The reduction and loss of AtSRT1 result in significant resistance to ABA, while overexpression of AtSRT1 leads to hypersensitivity to ABA, salt and osmotic stresses. SRT1/2 are involved in mediating transcriptional repression of ethylene signaling by decreasing the levels of H3K9 acetylation [93]. OsSRT1 participates in maintenance of genome stability and defense against DNA damage. Knockdown of *OsSRT1* triggers increased H3K9ac and decreased H3K9me2, resulting in oxidative burst, DNA fragmentation, and cell death, whereas overexpression of *OsSRT1* enhances tolerance to oxidative stress [94]. OsSRT1 represses glycolysis by both epigenetic regulation and deacetylating glycolytic GAPDH to inhibit its nuclear accumulation and moonlighting function as a transcriptional activator of glycolytic genes [95]. Taken together, *D. catenatum* SIR2 type HDACs would have a predominant role in energy metabolism.

Subcellular localization prediction

To investigate the functional compartmentation of DcHATs/DcHDACs, we predicted their subcellular localization through different software (Table 2). SLP-Local predictor showed the potential subcellular localization sites for most of DcHATs/DcHDACs with low reliability index (RI < 3), except for DcHAF1, which might be localized in the nucleus or cytosol with

higher reliability (RI = 6). However, Target P detected potential localization for nearly one half of these proteins with higher reliability (RC < 2), and all of them are localized in nucleus or cytosol. Uniprot program generated prediction results for only half of DcHATs and DcHDACs, including a SIR2-type HDAC, DcSRT2 with mitochondria localization as well as DcHAC1a/1b, DcHAG2, and DcHDA5a/5b/6/8/9/15/19 with nucleus localization. NES predictor (NetNES) detected the potential leucine-rich nuclear export signal (NES) for DcHATs and DcHDACs with a threshold value of 0.5. NES was found in most of DcHAT members except for DcHAG1, but only found in some DcHDAC members, such as DcHDA2b/6/9 and DcSRT2. The presence of the NES in 6 DcHATs and 4 DcHDACs indicates that they might perform the functions in both nucleus and cytosol. WoLF PSORT displayed low frequency values for DcHATs and DcHDACs; most of them were predicted with a major localization in the nucleus or cytosol, however, DcHAF1 generated the relatively close localization scores for nucleus (7) and cytosol (6), consistent with the dual localization predicted by other software (**Table 2**).

Promoter cis-element analysis

To detect the cis acting regulatory elements in DcHAT and DcHDAC gene promoter regions that determine the gene expression profiles, 2 kb sequences upstream of the ATG initiation codon were assessed via PlantCARE database [96]. Some phytohormone and stress-responsive cis-acting elements were selected to display (Fig. 5). According to function classification, these elements were mainly divided into two groups: □ phytohormone response elements including MeJA-responsive (82), abscisic acid responsive (27), gibberellin-responsive (16), auxin-responsive (14) and salicylic acid-responsive (10); □ stress response elements including anaerobic induction (28), low-temperature responsive (21), drought-inducibility (15), defense and stress responsive (10), anoxic specific inducibility (2) and wound-responsive (1). Overall, the four elements with the highest number were MeJA-responsive (82), anaerobic induction (28), abscisic acid responsive elements (27), and low-temperature responsive (21). Among these genes, *DcHDA2b* promoter only had a single predicted element, while DcHAG2 had maximal 18 elements. MeJA-responsive element (16/21) and anaerobic induction element (16/21) were found in most of DcHAT and DcHDAC promoter regions. Although experimental evidence is required to further check the correlation between cis-elements and gene expression response to different conditions, collected data revealed the involvement of DcHAT and DcHDAC genes in stress responses.

Expression profilings of DcHATs and DcHDACs in tissues and organs

To explore the tissue and organ-specificity of DcHATs and DcHDACs, their transcript levels were monitored in different plant tissues and organs, including leaf, root, green root tip, white part of root, stem, flower bud, sepal, labellum, pollinia, and gynostemium by RNA-seq data [97]. In DcHAT superfamily (Fig. 6A and **Additional file 2**), CBP members *DcHAC1a/1b* displayed similar expression pattern in vegetative organs and floral buds, but showed different patterns in mature floral organs, such as high expression of *DcHAC1a* and *DcHAC1b* in pollinia and root, respectively. Both MYST members *DcHAM1/2* had distinct expression profiles, such as DcHAM1 with intermediated expression but DcHAM2 lacking expression in detected tissues and organs. GNAT members *DcHAG1/2/3* and TAFII250 member *DcHAF1* displayed high expression in almost all the tissues and organs. In DcHDAC superfamily (Fig. 6B and **Additional file 2**), Class-I RPD3/HDA1 members had similar and intermediated expression patterns, except for *DcHDA6* with the highest expression in pollinia where DcHDA19/9 were absent. Class-IV members *DcHDA2a/2b* had similar but weak expression profiles. Class-II members displayed diverse expression patterns but had uniformly low expression in pollinia; *DcHDA8* harbored intermediated expression in almost all the organs; *DcHDA14*, *DcHDA15*, *DcHDA5a* seemingly had distinct expression levels in leaf, floral bud, and root/stem, respectively; *DcHDA5b* transcripts were absent in detected organs, indicating functional divergence of the *DcHDA5a/5b* genes. SIR2 members *DcSRT1/2* were also weakly expressed in all the organs except for intermediated expression of *DcSRT1* and *DcSRT12* in pollinia and labellum, respectively. On the other hand, HD2 members *DcHDT1/2* were strongly expressed in all the organs except for *DcHDT1* not in pollinia. These results indicated that DcHATs/DcHDACs have undergone the functional conservation and divergence during evolution.

Expression of DcHATs and DcHDACs in response to environmental stresses

To examine the responses of DcHATs and DcHDACs to cold stress, the expression levels of DcHATs and DcHDACs were evaluated through analyzing the RNA-seq data from the leaves of *D. catenatum* seedlings grown at 20 °C (control) and 0 °C for 20 h, respectively [98](Fig. 7 and **Additional file 3**). In DcHAT superfamily, the expression DcHAG1 transcription was markedly induced, but that of DcHAM1 was repressed by cold exposure. In DcHDAC superfamily, the transcription level of DcHDA14 was increased, but that of DcHDT1/2 was obviously decreased in responding to cold exposure.

To examine the responses of DcHATs and DcHDACs to drought stress, the transcriptional dynamics of DcHATs and DcHDACs were evaluated by analyzing the RNA-seq data from the leaves of *D. catenatum* seedlings under drought-recovery treatment [99] (Fig. 8 and **Additional file 4**). Briefly, the plants were irrigated on the 1st day, and kept dry for next 6 days, and rehydrated on the 8th day. Leaves were sampled at 18:30 on the 2nd (DR8), 7th (DR10), 8th (DR11), and 9th (DR15) days, respectively. The results suggested that 5-day drought treatment decreased the expressions of DcHAG1, DcHDA14, and DcHDA9, but increased the expression of DcHDA5a, and then rehydration restored the transcription of DcHAG1, DcHDA14, and DcHDA9 to the normal level.

To explore the response of DcHATs and DcHDACs to heat shock, the expression profiles of DcHATs and DcHDACs in the leaves of *D. catenatum* seedlings treated at 35 °C for different times were monitored by real-time quantitative RT-PCR (RT-qPCR) (Fig. 9). The results show that the expression levels of 4 DcHAT genes and 10 DcHDAC genes were significantly influenced by heat treatment, including DcHAM2 in MYST family, DcHAG1/2/3 in GNAT family, DcHDA6 /19/9 (Class I), DcHDA2a/2b (Class IV), DcHDA5a/5b (Class II) in RPD3/HDA1 family, and DcHDT1/2 in HD2 family. At 3 h after treatment (HAT), 8 genes were involved in early response to heat shock, including 5 upregulated genes and 3 downregulated genes. At 6 HAT, 7 genes were involved (6 upregulated genes and 1 downregulated genes). At 12 HAT, 5 genes were evidently induced, but no downregulated genes were detected. These indicate that the expression of DcHATs and DcHDACs are generally in positive response to heat shock. Notably, DcHAM2 and DcHDA5b transcripts were highly induced upon exposure to heat shock, but not detected in the expression profiles of different tissues and organs examined, indicating these two genes are mainly involved in heat shock response.

Discussion

Evolution and functional conservation of HAT and HDAC gene family

HATs/HDACs catalyzed histone acetylation-deacetylation interconversions realize the switch between permissive (open) and repressive (close) states of chromatin, leading to induction/silencing and upregulation/downregulation of gene expression in response to developmental cues and environmental stimuli. Genome-wide identification of HATs/HDACs have been documented in some representative plant species, such as Arabidopsis, sweet orange, apple, tomato, rice, maize, and liverwort. Unexpectedly, HAG family in apple, orange, and tomato was reported to contain 50, 45, and 26 members, respectively [9, 10, 12], far more than that in other reported species. So, we further checked and screened the true HAG paralogs through more strict criteria satisfying the first hit for each other in reciprocal blast and inclusion of Acetyltransf_1/Elp3 domain combination. eventually, we only detected 5, 4, and 3 HAGs in apple, orange, and tomato, respectively. Intriguingly, an ideal grain-weight QTL in rice has been identified and verified as a novel HAT member, OsglHAT1 (Os06g44100) with Acetyltransf_1 domain but lack of Elp3 domain, which further broads the scope of HATs and also provides a single target for directional yield improvement breeding [100]. Thus, it is logical to speculate that any protein containing Acetyltransf_1 domain might harbor HAT activity. The epiphytic orchid plant *D. catenatum* has highly specialized organogenesis and unique living mode, but no HATs/HDACs homologs were reported so far. In present study, we identified 8 HATs and 14 HDACs in *D. catenatum*, as well as 7 HATs and 13 HDACs in its closely relative *Phalaenopsis equstris* (Fig. 10). Overall, the gene number in each HAT/HDAC family remains relatively stable throughout the green plant lineage during evolution, resulting in gene copy number that is not positively correlated with genome size. This result indicated that HATs/HDACs associated with histone acetylation/deacetylation have functional conservation and dosage stability during evolution, and genome rearrangement and gene deletion might happen to offset gene dosage effect induced by the polyploidization events during evolution.

Examination on acetylated proteins in rice suspension cells shows lysine acetylation on nuclear proteins only occupies 17.2%, and acetylation on nonhistone proteins accounts for the majority [101]. In fact, lysine acetylation on nonhistone proteins as the ancestral function first happened in prokaryote. In bacteria, protein acetylation is widely involved in the regulation of central and secondary metabolism, virulence, transcription, and translation [102]. More than 70% of the acetylated proteins are metabolic enzymes and translation regulators in *Escherichia coli* [103]. Lysine acetylation can control central metabolic metabolism by directly switching off enzyme activity [104]. Acetylation is involved in tight regulation of acetyl-CoA synthetase activity necessary for maintenance of energy homeostasis in bacteria [102]. So, protein acetylation is an ancient and widespread strategy for protein activity regulation, especially on the aspect of energy metabolism [104], which is directly associated with survival of organisms and rapid environmental adaption. In eukaryote, DNA wraps around the histone octamer to assemble into nucleosome as the basic unit of chromatin, and lysine acetylation acquires novel role to occur at histone tails, leading to modification of chromatin structure and regulation of gene expression on epigenetic level. In fact, acetylation on nonhistone and histone can be linked together by acetyl-CoA, which is a hub metabolite and can supply acetyl group for both. Cells sense their metabolic state through monitoring the levels of the key indicator, acetyl-CoA. Disruption of cytosolic acetyl-CoA carboxylase *ACC1* leads to elevated level of acetyl-CoA and increased deposition of histone acetylation predominantly at H3K27ac; comprehensive analysis suggests that H3K27ac is an essential link between cytosolic acetyl-CoA level and gene expression in response to the dynamic metabolic environments in plants [105, 106].

Subcellular localization of HAT and HDAC proteins

HAT and HDAC proteins not only modify the histone tails to change chromatin status on genome level but also catalyze nonhistone proteins to directly regulate the activities of specific targets, and the diversity of substrate type results in the divergence of subcellular localization of HAT and HDAC proteins. A proportion of HAT/HDAC proteins are exclusively localized in the nucleus, such as Arabidopsis GCN5, HAM2, HDA19 and rice HDT701 [90, 107]. However, distinct proteins have different domain preference even in nucleus. AtHAG1/2 and AtHAM1/2 are rich at the periphery of the nucleolus [108]. AtHD1 is localized in the euchromatic regions and excluded from the nucleolus, different from AtHD2 [109]. Microbial-associated molecular pattern (MAMP)-activated MAP kinase MPK3 directly interacts with and phosphorylates HD2B, leading to relocalization of HD2B from the nucleolus to the nucleoplasm and global genome-wide shifts in the H3K9 acetylation landscape [57]. In present study, the nucleus localization of about a half of DcHATs (3/8) and DcHDACs (9/14) was successfully predicted by Uniprot or Wolf PSORT. Some members have cytoplasm-predominant localization or cytoplasm/nucleus dual localization. Arabidopsis RPD3 type Class II HDACs, HDA5, HDA8, and HDA18 are localized in the cytoplasm [107]. AtHDA15 shuttles from the cytoplasm to the nucleus in response to light [110]. Transient expression in Arabidopsis protoplasts showed the dual localization of OsHAC701, OsHAG702, and OsHAG704 [6]. Here, subcellular localization prediction by Wolf PSORT indicated that most of DcHATs might localize in both the nucleus and cytoplasm, suggesting a potential shuttling process between these compartments. Some members localize in mitochondrial or chloroplast. Arabidopsis SRT2 resides at mitochondrial and participates in fine-tuning energy metabolism [36]. Similarly, DcSRT2 was predicted to have mitochondrial localization. So, HAT and HDAC proteins fulfill diverse roles to realize broad and fine regulation on both genome-wide and specific-locus levels partially by functional compartmentation.

Roles of HATs and HDACs in developmental regulation and stress response

HATs and HDACs usually function with other cofactors and crosstalk with different pathways. HAT/HDAC protein can act as a subunit of multiprotein complex. Arabidopsis HD2C deacetylase interacts with SWI/SNF chromatin remodeling complex to mediate heat stress response [111]. HAT/HDAC protein together with transcription factor functions as the most general regulatory combination. AP2 recruits the co-repressor TOPLESS and the histone deacetylase HDA19 to regulate flower development by controlling the expression territories of numerous floral organ identity genes [112]. HDA19 interact with HSL1 to directly repress seed maturation gene expression during germination [113]. HDA15 together with PIF3 and PIF1 is involved in repressing chlorophyll biosynthesis and seed germination, respectively [79, 80]. HATs/HDACs associated with histone acetylation status crosstalk with phytohormone signal pathways. Ethylene induces histone acetylation in both genome-wide level and a group of ethylene regulated genes [114–116]. The key jasmonate (JA) signaling repressor JAZ1 interacts with two

ethylene-stabilized factors EIN3/EIL1, recruits HDA6 to co-repress transcriptional activity of EIN3/EIL1 [117]. HATs/HDACs interplay with each other or other epigenetic modification. HD2C can interact with HDA6 to regulate gene expression; ABA-responsive genes ABI1/2 with enhanced expression in *hda6* or/and *hd2c* single and double mutants are associated with increased histone H3K9/K14 acetylation and decreased H3K9 dimethylation (H3K9me2) [89]. FVE/MSI4 interacts with HDA6 and the histone demethylase FLD to regulate flowering time by repressing FLC through decreasing histone H3K4me3 and H3 acetylation [69]. Histone demethylases LDL1 and LDL2 interact with HDA6 and CCA1/LHY co-repress TOC1 expression, involved in regulating circadian rhythms [55].

HATs/HDACs are involved in plant responses to various abiotic and biotic stresses. Class-I HDAC (HDA19) and class-II HDACs (HDA5/14/15/18) execute different mechanisms underlying salinity stress responses; *hda19* single mutant and *hda5/14/15/18* plant exhibit more tolerance and sensitivity to salt stress, respectively [63]. Drought stress significantly increases the expression of a subset of HATs (*OsHAC703*, *OsHAG703*, *OsHAF701* and *OsHAM701*) and global acetylation level in rice [118]. Here we observed that 5-day drought treatment decreased the expression of HAT member *DcHAG1* and HDAC members *DcHDA14/DcHDA9*, indicating that histone acetylation and deacetylation in distinct loci may contribute to the similar stress response. In rice, cold treatment leads to decreased expression of *OsHDA704/OsHDA712/OsSRT701* but increased expression of OsHDA702 [119]. In *D. catenatum*, we found that cold exposure induced the expression of HAT members *DcHAG1* and HDAC members *DcHDA14*, but repressed the expression of HAT members *DcHAM1* and HDAC members *DcHDT1/2*, indicating that different DcHAT/DcHDAC families might take charge of distinct responses to cold stress for fine-tuning regulation. Furthermore, the promoter region of *DcHAG1* was found to contain four low-temperature responsive elements, supporting its significance in cold response. It has been demonstrated that heat stress at 38 °C for 3 h increases the expression of *AtHDA6/7/5/8/14* in Arabidopsis [18]. The *hda19-1* mutant is sensitive to high temperature, and displays abnormal cotyledon morphogenesis at 29 °C, compared with normal development at 25 °C [120]. In present study, high temperature treatment caused the dynamic expression changes of 50% of DcHATs and 71% of DcHDACs, which were upregulated at least at one time point. This result suggested that histone acetylation/deacetylation are widely involved in heat stress response for genome-wide programing of downstream gene expression. Defense hormone JA can induce the expression of *HDA6* and *HDA19* in Arabidopsis [121]. But in *D. catenatum*, exogenous application of JA repressed the expression of *DcHAG2*, *DcHDT1/2* and *DcHDA15* (**Additional file 5**), indicating JA has different effects on histone acetylation in different species. Additionally, HDA19 participates in the repression of SA-mediated basal defense responses, and loss of *HDA19* enhances SA content and the expression of SA accumulation-related genes and PR genes, thereby causing increased resistance to *Pseudomonas syringae* [122]. In rice, *HDT701* negatively regulates innate immunity by modulating histone H4 acetylation of defense-related genes, and overexpression and silencing of *HDT701* leads to more susceptibility and resistance to the rice pathogens *Magnaporthe oryzae* and *Xanthomonas oryzae* pv *oryzae*, respectively [123]. Southern Blight caused by necrotrophic pathogen *Sclerotium delphinii* is a disaster disease of *D. catenatum* [124], but its infection had no obvious influence at the transcriptional level of DcHATs/DcHDACs (**Additional file 5**). It is worth investigating their changes on translational and posttranslational levels. On the other hand, the pathogen may promote disease by manipulating host histone acetylation during infection. The soybean pathogen *Phytophthora sojae* can produce the cytoplasmic effector PsAvh23, which binds to ADA2 subunit of the HAT complex SAGA to disrupt ADA2-GCN5 module formation and subsequently suppresses the expression of defense genes by decreasing GCN5-mediated H3K9ac levels, and increases plant susceptibility [125]. The sugar beet cyst nematode (*Heterodera schachtii*) 32E03 effector interacts with histone deacetylase HDT1 and inhibits its activities, regulates rRNA gene dosage, promote cyst nematode parasitism [126]. Therefore, identification of HAT/HDAC candidates directly involving plant-pathogen interactions will provide key targets for directed genetic improvement and accelerate crop resistance breeding.

Conclusions

In present study, we identified 8 HATs and 14 HDACs *in D. catenatum* at the genome-wide level, and classified them into different families based on the phylogenetic reconstruction using well-defined homologs of model plants Arabidopsis and rice as references. Furthermore, promoter cis-element, subcellular localization, tissue and organ expression profiles, transcriptional responses to abiotic and biotic stresses of *D. catenatum* HATs and HDACs were analyzed. Our results shed light on the

involvement of DcHATs/DcHDACs in developmental programs and stress responses, and provide comprehensive information for further functional dissection of HATs/HDACs in orchids.

Methods

Identification of HAT and HDAC members in D. catenatum

The genome, CDS and protein sequences of both HATs and HDACs of *Arabidopsis thaliana* and rice were retrieved from TAIR (The Arabidopsis Information Resource, https://www.arabidopsis.org/) and RGAP (Rice Genome Annotation Project, http://rice.plantbiology.msu.edu/) official websites, respectively. The protein sequences of HATs and HDACs of Arabidopsis and rice were used as queries to search for the homologs in the *D. catenatum* genome using the BLASTp algorithm in the NCBI browser (blast.ncbi.nlm.nih.gov/Blast.cgi). The hits of all HAT and HDAC proteins were analyzed for recognizable domains using NCBI Batch Web CD-Search Tool (https://www.ncbi.nlm.nih.gov/Structure/bwrpsb/bwrpsb.cgi) and HMMER based SMART mode (http://smart.embl-heidelberg.de). Reciprocal BLAST was used for further confirmation.

Alignments and phylogenetic analyses

HAT and HDAC proteins were aligned using Clustalw [127], and phylogenetic analysis was performed using MEGA7 program [128]. The full-length amino acid sequences of HATs and HDACs were used for constructing neighbor-joining (NJ) trees with the following settings: pairwise deletion option for gaps/missing data treatment; *p*-distance method for Substitution model; and bootstrap test of 1000 replicates for internal branch reliability.

Gene Structure and domain organization analysis

Exon–intron gene structure schematics of HAT and HDAC genes were analyzed by online program Gene Structure Display Server GSDS 2.0 (http://gsds.cbi.pku.edu.cn/) [129]. The domain organization of HAT and HDAC proteins were analyzed using SMART and Pfam databases.

Subcellular localization prediction and cis element analysis

The subcellular localization of DcHAT/DcHDAC proteins were predicted via SLP-Local (http://sunflower.kuicr.kyoto-u.ac.jp/~smatsuda/slplocal.html) [130], WoLF PSORT II (https://www.genscript.com/wolf-psort.html), Uniprot (http://uniprot.org). TargetP-2.0 server (http://www.cbs.dtu.dk/services/TargetP/) [131], and NetNES 1.1 server (http://www.cbs.dtu.dk/services/NetNES/) [132]. The key cis-acting elements in DcHAT/DcHDAC promoter regions (2 kb upstream of ATG) were searched against the online prediction tool PlantCARE database (http://bioinformatics.psb.ugent.be/webtools/plantcare/html/) and were displayed through TBtools [133].

In silico analysis of transcriptome data

For spatio-temporal expression of DcHAT and DcHDAC genes, the raw RNA-seq reads of different tissue and organs in *D. catenatum* were downloaded from NCBI, including leaf (SRR4431601), root (SRR5722140), Green root tip (SRR4431599), white part of root (SRR4431598), stem (SRR4431600), flower bud (SRR4431603), sepal (SRR4431597), labellum (SRR4431602), pollinia (SRR5722145) and gynostemium (SRR4431596) [97]. For drought stress and recovery experiment in 8-month-old *D. catenatum* plants [99], irrigation was performed on the 1st day, omitted from the 2nd to the 7th day, and resumed on the 8th day, watering every 2 days at 15:30. Consequently, the raw RNA-seq reads were obtained from the leaves that were harvested at 18:30 on the 2nd [DR6 (SRR7223298)], 7th [(DR8 (SRR7223300)], 8th [DR10 (SRR7223296)], and 9th [DR15 (SRR7223297)] day, respectively. For cold stress experiment, the raw RNA-seq reads of leaves under 20 °C control condition (SRR3210630, SRR3210635 and SRR3210636) and 0 °C treatment (SRR3210613, SRR3210621 and SRR3210626) for 20 h were obtained from NCBI [98]. Reads of all the samples were aligned to Dendrobium reference genome via HISAT package [134]. The mapped reads of each sample were assembled and gene expression levels were calculated by the FPKM method via StringTie [135]. Heatmap was generated via TBtools software [133].

Plant material and high temperature treatment

D. catenatum cultivar “Jingpin NO. 1” (Zhejiang Province, China) was grown in green chamber at 20 °C under a 12 h light/12 h dark regime. 1-year-old seedlings were exposed at 35 ℃ heat shock for indicated time (3 h, 6 h and 12 h), compared with the control plants at 20 ℃. Subsequently, the leaves were collected and frozen in liquid nitrogen for RNA extraction.

Real-Time quantitative RT-PCR (RT-qPCR)

Total RNA was extracted via TRIzol reagent (Invitrogen, USA) followed by RNase-free DNase I treatment. First strand cDNA synthesis was performed via PrimerScript RT Enzyme Mix I kit (TaKaRa, Japan), according to the manufacturer’s instructions. RT-qPCR reaction mixture (10 μl) was prepared according to the manual of SYBR® Premix Ex Taq™ II (Tli RNaseH Plus) kit (TaKaRa, Japan). Then the reaction was carried out on CFX96 Touch™ Real-Time PCR Detection System (BIO-RAD, USA) in three technical replicates for each biological triplicate using the primers listed in **Additional file 6**. The reaction condition was set as the following procedure: 94 ℃ for 3 m, 40 cycles of 94 °C for 20 s, 60 ℃ for 20 s, 72℃ for 20 s. *DcACTIN* was used as the internal reference. The relative expression level was calculated with $2^{-\Delta\Delta CT}$ method.

Abbreviations

AG: AGAMOUS; CBP: cAMP-responsive element-binding protein; GCN5: GENERAL CONTROL NON-REPRESSIBLE 5; GNAT: GCN5-related N-terminal acetyltransferase; HD2: histone deacetylase 2; H3K4me3: H3K4 trimethylation; H3K9me2: H3K9 dimethylation; HAT: histone acetyltransferase; HDAC: histone deacetylase; JA: jasmonate; MAMP: Microbial-associated molecular pattern; MYST: MOZ-Ybf2/Sas3-Sas2-Tip60; PIF3: PHYTOCHROME INTERACTING FACTOR3; PLT: PLETHORA; PRC2: Polycomb repressive complex 2; RPD3: reduced potassium dependency 3; RT-qPCR: Real-Time quantitative RT-PCR; SA: salicylic acid; SIR2: silent information regulator 2;TAF: TATA-binding protein Associated Factor; WUS: WUSCHEL

Declarations

Ethics approval and consent to participate

The *D. catenatum* used in this study is a commercial cultivar "Jingpin NO. 1", which was cultivated by Prof Jinping Si (Zhejiang A&F University), was authorized by Zhejiang Province with Breed NO. Zhe R-SV-DO-015-2014. It does not require ethical approval.

Consent to publish

Not applicable.

Availability of data and materials

All data generated or analyzed during this study are included in this published article and its Additional files. The datasets generated and analyzed during the current study are available from the corresponding author on reasonable request.

Competing interests

The authors declare that they have no competing interests.

Funding

This work was funded by National Key R&D Program of China (2017YFC1702201), National Natural Science Foundation of China (31870310), Scientific R&D Foundation for Talent Start-up Project of Zhejiang A&F University (2017FR035), and the State Key Laboratory of Subtropical Silviculture (ZY20180206). The funding agencies were not involved in the design of the study and collection, analysis, and interpretation of data and in writing the manuscript.

Authors' contributions

DHC and JPS planned and designed the research. WWJ and DHQ performed the experiments. DHC, WWJ, and JLT analyzed the data. DHC and JPS wrote the article. All the authors approved the manuscript.

Acknowledgements

We thank editors and reviewers for the careful reading and valuable comments.

Authors' Information

[1] State Key Laboratory of Subtropical Silviculture, SFGA Engineering Research Center for *Dendrobium catenatum* (*D. officinale*), Zhejiang A&F University, Lin'an, Hangzhou, Zhejiang 311300, China

References

1. Wang Z, Zang C, Cui K, Schones DE, Barski A, Peng W, Zhao K. Genome-wide mapping of HATs and HDACs reveals distinct functions in active and inactive genes. Cell. 2009;138(5):1019–31.
2. Liu X, Yang S, Yu CW, Chen CY, Wu K. Histone Acetylation and Plant Development. The Enzymes. 2016;40:173–99.
3. Lu L, Chen X, Sanders D, Qian S, Zhong X. High-resolution mapping of H4K16 and H3K23 acetylation reveals conserved and unique distribution patterns in Arabidopsis and rice. Epigenetics. 2015;10(11):1044–53.
4. Mahrez W, Arellano MS, Moreno-Romero J, Nakamura M, Shu H, Nanni P, Kohler C, Gruissem W, Hennig L. H3K36ac Is an Evolutionary Conserved Plant Histone Modification That Marks Active Genes. Plant physiology. 2016;170(3):1566–77.
5. Pandey R, Muller A, Napoli CA, Selinger DA, Pikaard CS, Richards EJ, Bender J, Mount DW, Jorgensen RA. Analysis of histone acetyltransferase and histone deacetylase families of Arabidopsis thaliana suggests functional diversification of chromatin modification among multicellular eukaryotes. Nucleic acids research. 2002;30(23):5036–55.
6. Liu X, Luo M, Zhang W, Zhao J, Zhang J, Wu K, Tian L, Duan J. Histone acetyltransferases in rice (Oryza sativa L.): phylogenetic analysis, subcellular localization and expression. BMC plant biology. 2012;12:145.
7. Hu Y, Qin F, Huang L, Sun Q, Li C, Zhao Y, Zhou DX. Rice histone deacetylase genes display specific expression patterns and developmental functions. Biochem Biophys Res Commun. 2009;388(2):266–71.
8. Aquea F, Timmermann T, Arce-Johnson P. Analysis of histone acetyltransferase and deacetylase families of Vitis vinifera. Plant physiology biochemistry: PPB. 2010;48(2–3):194–9.
9. Aiese Cigliano R, Sanseverino W, Cremona G, Ercolano MR, Conicella C, Consiglio FM. Genome-wide analysis of histone modifiers in tomato: gaining an insight into their developmental roles. BMC Genomics. 2013;14:57.
10. Xu J, Xu H, Liu Y, Wang X, Xu Q, Deng X. Genome-wide identification of sweet orange (Citrus sinensis) histone modification gene families and their expression analysis during the fruit development and fruit-blue mold infection process. Frontiers in plant science. 2015;6:607.
11. Peng M, Ying P, Liu X, Li C, Xia R, Li J, Zhao M. Genome-Wide Identification of Histone Modifiers and Their Expression Patterns during Fruit Abscission in Litchi. Frontiers in plant science. 2017;8:639.
12. Fan S, Wang J, Lei C, Gao C, Yang Y, Li Y, An N, Zhang D, Han M. Identification and characterization of histone modification gene family reveal their critical responses to flower induction in apple. BMC plant biology. 2018;18(1):173.
13. Chu J, Chen Z. Molecular identification of histone acetyltransferases and deacetylases in lower plant Marchantia polymorpha. Plant physiology biochemistry: PPB. 2018;132:612–22.
14. Ma X, Zhang C, Zhang B, Yang C, Li S. Identification of genes regulated by histone acetylation during root development in Populus trichocarpa. BMC Genomics. 2016;17:96.
15. Yang C, Shen W, Chen H, Chu L, Xu Y, Zhou X, Liu C, Chen C, Zeng J, Liu J, et al. Characterization and subcellular localization of histone deacetylases and their roles in response to abiotic stresses in soybean. BMC plant biology. 2018;18(1):226.

16. Kumar V, Singh B, Singh SK, Rai KM, Singh SP, Sable A, Pant P, Saxena G, Sawant SV. Role of GhHDA5 in H3K9 deacetylation and fiber initiation in Gossypium hirsutum. The Plant journal: for cell molecular biology. 2018;95(6):1069–83.
17. Imran M, Shafiq S, Farooq MA, Naeem MK, Widemann E, Bakhsh A, Jensen KB, Wang RR. **Comparative Genome-wide Analysis and Expression Profiling of Histone Acetyltransferase (HAT) Gene Family in Response to Hormonal Applications, Metal and Abiotic Stresses in Cotton**. *International journal of molecular sciences* 2019, 20(21).
18. Alinsug MV, Yu CW, Wu K. Phylogenetic analysis, subcellular localization, and expression patterns of RPD3/HDA1 family histone deacetylases in plants. BMC plant biology. 2009;9:37.
19. Xu CR, Liu C, Wang YL, Li LC, Chen WQ, Xu ZH, Bai SN. Histone acetylation affects expression of cellular patterning genes in the Arabidopsis root epidermis. Proc Natl Acad Sci USA. 2005;102(40):14469–74.
20. Chen WQ, Li DX, Zhao F, Xu ZH, Bai SN. One additional histone deacetylase and 2 histone acetyltransferases are involved in cellular patterning of Arabidopsis root epidermis. Plant Signal Behav. 2016;11(2):e1131373.
21. Kornet N, Scheres B. Members of the GCN5 histone acetyltransferase complex regulate PLETHORA-mediated root stem cell niche maintenance and transit amplifying cell proliferation in Arabidopsis. Plant Cell. 2009;21(4):1070–9.
22. Kim JY, Yang W, Forner J, Lohmann JU, Noh B, Noh YS. **Epigenetic reprogramming by histone acetyltransferase HAG1/AtGCN5 is required for pluripotency acquisition in Arabidopsis**. *The EMBO journal* 2018, 37(20).
23. Tanaka M, Kikuchi A, Kamada H. The Arabidopsis histone deacetylases HDA6 and HDA19 contribute to the repression of embryonic properties after germination. Plant physiology. 2008;146(1):149–61.
24. Bertrand C, Bergounioux C, Domenichini S, Delarue M, Zhou DX. Arabidopsis histone acetyltransferase AtGCN5 regulates the floral meristem activity through the WUSCHEL/AGAMOUS pathway. J Biol Chem. 2003;278(30):28246–51.
25. Zeng X, Gao Z, Jiang C, Yang Y, Liu R, He Y. HISTONE DEACETYLASE 9 Functions with Polycomb Silencing to Repress FLOWERING LOCUS C Expression. Plant physiology. 2020;182(1):555–65.
26. Forestan C, Farinati S, Rouster J, Lassagne H, Lauria M, Dal Ferro N, Varotto S. Control of Maize Vegetative and Reproductive Development, Fertility, and rRNAs Silencing by HISTONE DEACETYLASE 108. Genetics. 2018;208(4):1443–66.
27. Guo JE, Hu Z, Li F, Zhang L, Yu X, Tang B, Chen G. Silencing of histone deacetylase SlHDT3 delays fruit ripening and suppresses carotenoid accumulation in tomato. Plant science: an international journal of experimental plant biology. 2017;265:29–38.
28. Guo JE, Hu Z, Yu X, Li A, Li F, Wang Y, Tian S, Chen G. A histone deacetylase gene, SlHDA3, acts as a negative regulator of fruit ripening and carotenoid accumulation. Plant cell reports. 2018;37(1):125–35.
29. Guo JE, Hu Z, Zhu M, Li F, Zhu Z, Lu Y, Chen G. The tomato histone deacetylase SlHDA1 contributes to the repression of fruit ripening and carotenoid accumulation. Scientific reports. 2017;7(1):7930.
30. Benhamed M, Bertrand C, Servet C, Zhou DX. Arabidopsis GCN5, HD1, and TAF1/HAF2 interact to regulate histone acetylation required for light-responsive gene expression. Plant Cell. 2006;18(11):2893–903.
31. Fina JP, Casati P. HAG3, a Histone Acetyltransferase, Affects UV-B Responses by Negatively Regulating the Expression of DNA Repair Enzymes and Sunscreen Content in Arabidopsis thaliana. Plant Cell Physiol. 2015;56(7):1388–400.
32. Fina JP, Masotti F, Rius SP, Crevacuore F, Casati P. HAC1 and HAF1 Histone Acetyltransferases Have Different Roles in UV-B Responses in Arabidopsis. Frontiers in plant science. 2017;8:1179.
33. Campi M, D'Andrea L, Emiliani J, Casati P. Participation of chromatin-remodeling proteins in the repair of ultraviolet-B-damaged DNA. Plant physiology. 2012;158(2):981–95.
34. Li S, Lin YJ, Wang P, Zhang B, Li M, Chen S, Shi R, Tunlaya-Anukit S, Liu X, Wang Z, et al. The AREB1 Transcription Factor Influences Histone Acetylation to Regulate Drought Responses and Tolerance in Populus trichocarpa. Plant Cell. 2019;31(3):663–86.
35. Ma X, Zhang B, Liu C, Tong B, Guan T, Xia D. Expression of a populus histone deacetylase gene 84KHDA903 in tobacco enhances drought tolerance. Plant science: an international journal of experimental plant biology. 2017;265:1–11.

36. Konig AC, Hartl M, Pham PA, Laxa M, Boersema PJ, Orwat A, Kalitventseva I, Plochinger M, Braun HP, Leister D, et al. The Arabidopsis class II sirtuin is a lysine deacetylase and interacts with mitochondrial energy metabolism. Plant physiology. 2014;164(3):1401–14.
37. Hao Y, Wang H, Qiao S, Leng L, Wang X. Histone deacetylase HDA6 enhances brassinosteroid signaling by inhibiting the BIN2 kinase. Proc Natl Acad Sci USA. 2016;113(37):10418–23.
38. Si JP, Zhang Y, Luo YB, Liu JJ, Liu ZJ. [Herbal textual research on relationship between Chinese medicine"Shihu" (Dendrobium spp.) and "Tiepi Shihu" (D. catenatum)]. Zhongguo Zhong yao za zhi = Zhongguo zhongyao zazhi = China journal of Chinese materia medica. 2017;42(10):2001–5.
39. Yan L, Wang X, Liu H, Tian Y, Lian J, Yang R, Hao S, Wang X, Yang S, Li Q, et al. The Genome of Dendrobium officinale Illuminates the Biology of the Important Traditional Chinese Orchid Herb. Molecular plant. 2015;8(6):922–34.
40. Cheng J, Dang PP, Zhao Z, Yuan LC, Zhou ZH, Wolf D, Luo YB. An assessment of the Chinese medicinal Dendrobium industry: Supply, demand and sustainability. J Ethnopharmacol. 2019;229:81–8.
41. Tang H, Zhao T, Sheng Y, Zheng T, Fu L, Zhang Y. Dendrobium officinale Kimura et Migo: A Review on Its Ethnopharmacology, Phytochemistry, Pharmacology, and Industrialization. Evidence-based complementary alternative medicine: eCAM. 2017;2017:7436259.
42. Deng W, Liu C, Pei Y, Deng X, Niu L, Cao X. Involvement of the histone acetyltransferase AtHAC1 in the regulation of flowering time via repression of FLOWERING LOCUS C in Arabidopsis. Plant physiology. 2007;143(4):1660–8.
43. Han SK, Song JD, Noh YS, Noh B. Role of plant CBP/p300-like genes in the regulation of flowering time. The Plant journal: for cell molecular biology. 2007;49(1):103–14.
44. Jin H, Choi SM, Kang MJ, Yun SH, Kwon DJ, Noh YS, Noh B. Salicylic acid-induced transcriptional reprogramming by the HAC-NPR1-TGA histone acetyltransferase complex in Arabidopsis. Nucleic acids research. 2018;46(22):11712–25.
45. Dhalluin C, Carlson JE, Zeng L, He C, Aggarwal AK, Zhou MM. Structure and ligand of a histone acetyltransferase bromodomain. Nature. 1999;399(6735):491–6.
46. Vlachonasios KE, Thomashow MF, Triezenberg SJ. Disruption mutations of ADA2b and GCN5 transcriptional adaptor genes dramatically affect Arabidopsis growth, development, and gene expression. Plant Cell. 2003;15(3):626–38.
47. Servet C, Conde e Silva N, Zhou DX. Histone acetyltransferase AtGCN5/HAG1 is a versatile regulator of developmental and inducible gene expression in Arabidopsis. Molecular plant. 2010;3(4):670–7.
48. Xing J, Wang T, Liu Z, Xu J, Yao Y, Hu Z, Peng H, Xin M, Yu F, Zhou D, et al. GENERAL CONTROL NONREPRESSED PROTEIN5-Mediated Histone Acetylation of FERRIC REDUCTASE DEFECTIVE3 Contributes to Iron Homeostasis in Arabidopsis. Plant physiology. 2015;168(4):1309–20.
49. Wang T, Xing J, Liu X, Liu Z, Yao Y, Hu Z, Peng H, Xin M, Zhou DX, Zhang Y, et al: **Histone acetyltransferase general control non-repressed protein 5** (**GCN5**) **affects the fatty acid composition of Arabidopsis thaliana seeds by acetylating fatty acid desaturase3** (**FAD3**). *The Plant journal: for cell and molecular biology* 2016, **88**(5):794–808.
50. Wang T, Xing J, Liu X, Yao Y, Hu Z, Peng H, Xin M, Zhou DX, Zhang Y, Ni Z. GCN5 contributes to stem cuticular wax biosynthesis by histone acetylation of CER3 in Arabidopsis. J Exp Bot. 2018;69(12):2911–22.
51. Hu Z, Song N, Zheng M, Liu X, Liu Z, Xing J, Ma J, Guo W, Yao Y, Peng H, et al. Histone acetyltransferase GCN5 is essential for heat stress-responsive gene activation and thermotolerance in Arabidopsis. The Plant journal: for cell molecular biology. 2015;84(6):1178–91.
52. Zheng M, Liu X, Lin J, Liu X, Wang Z, Xin M, Yao Y, Peng H, Zhou DX, Ni Z, et al. Histone acetyltransferase GCN5 contributes to cell wall integrity and salt stress tolerance by altering the expression of cellulose synthesis genes. The Plant journal: for cell molecular biology. 2019;97(3):587–602.
53. Watkins JF, Sung P, Prakash L, Prakash S. The Saccharomyces cerevisiae DNA repair gene RAD23 encodes a nuclear protein containing a ubiquitin-like domain required for biological function. Molecular cellular biology. 1993;13(12):7757–65.

54. Bertrand C, Benhamed M, Li YF, Ayadi M, Lemonnier G, Renou JP, Delarue M, Zhou DX. Arabidopsis HAF2 gene encoding TATA-binding protein (TBP)-associated factor TAF1, is required to integrate light signals to regulate gene expression and growth. J Biol Chem. 2005;280(2):1465–73.
55. Lee K, Seo PJ. The HAF2 protein shapes histone acetylation levels of PRR5 and LUX loci in Arabidopsis. Planta. 2018;248(2):513–8.
56. Jenuwein T, Allis CD. Translating the histone code. Science. 2001;293(5532):1074–80.
57. Latrasse D, Benhamed M, Henry Y, Domenichini S, Kim W, Zhou DX, Delarue M. The MYST histone acetyltransferases are essential for gametophyte development in Arabidopsis. BMC plant biology. 2008;8:121.
58. Xiao J, Zhang H, Xing L, Xu S, Liu H, Chong K, Xu Y. Requirement of histone acetyltransferases HAM1 and HAM2 for epigenetic modification of FLC in regulating flowering in Arabidopsis. Journal of plant physiology. 2013;170(4):444–51.
59. Steggerda SM, Paschal BM. Regulation of nuclear import and export by the GTPase Ran. Int Rev Cytol. 2002;217:41–91.
60. Tian L, Chen ZJ. Blocking histone deacetylation in Arabidopsis induces pleiotropic effects on plant gene regulation and development. Proc Natl Acad Sci USA. 2001;98(1):200–5.
61. Tian L, Wang J, Fong MP, Chen M, Cao H, Gelvin SB, Chen ZJ. Genetic control of developmental changes induced by disruption of Arabidopsis histone deacetylase 1 (AtHD1) expression. Genetics. 2003;165(1):399–409.
62. Ueda M, Matsui A, Nakamura T, Abe T, Sunaoshi Y, Shimada H, Seki M. Versatility of HDA19-deficiency in increasing the tolerance of Arabidopsis to different environmental stresses. Plant Signal Behav. 2018;13(8):e1475808.
63. Ueda M, Matsui A, Tanaka M, Nakamura T, Abe T, Sako K, Sasaki T, Kim JM, Ito A, Nishino N, et al. The Distinct Roles of Class I and II RPD3-Like Histone Deacetylases in Salinity Stress Response. Plant physiology. 2017;175(4):1760–73.
64. Jang IC, Pahk YM, Song SI, Kwon HJ, Nahm BH, Kim JK. Structure and expression of the rice class-I type histone deacetylase genes OsHDAC1-3: OsHDAC1 overexpression in transgenic plants leads to increased growth rate and altered architecture. The Plant journal: for cell molecular biology. 2003;33(3):531–41.
65. Chung PJ, Kim YS, Jeong JS, Park SH, Nahm BH, Kim JK. The histone deacetylase OsHDAC1 epigenetically regulates the OsNAC6 gene that controls seedling root growth in rice. The Plant journal: for cell molecular biology. 2009;59(5):764–76.
66. Cheng X, Zhang S, Tao W, Zhang X, Liu J, Sun J, Zhang H, Pu L, Huang R, Chen T. INDETERMINATE SPIKELET1 Recruits Histone Deacetylase and a Transcriptional Repression Complex to Regulate Rice Salt Tolerance. Plant physiology. 2018;178(2):824–37.
67. Luo M, Yu CW, Chen FF, Zhao L, Tian G, Liu X, Cui Y, Yang JY, Wu K. Histone deacetylase HDA6 is functionally associated with AS1 in repression of KNOX genes in arabidopsis. PLoS Genet. 2012;8(12):e1003114.
68. Li DX, Chen WQ, Xu ZH, Bai SN. HISTONE DEACETYLASE6-Defective Mutants Show Increased Expression and Acetylation of ENHANCER OF TRIPTYCHON AND CAPRICE1 and GLABRA2 with Small But Significant Effects on Root Epidermis Cellular Pattern. Plant physiology. 2015;168(4):1448–58.
69. Yu CW, Chang KY, Wu K. Genome-Wide Analysis of Gene Regulatory Networks of the FVE-HDA6-FLD Complex in Arabidopsis. Frontiers in plant science. 2016;7:555.
70. Tessadori F, van Zanten M, Pavlova P, Clifton R, Pontvianne F, Snoek LB, Millenaar FF, Schulkes RK, van Driel R, Voesenek LA, et al. Phytochrome B and histone deacetylase 6 control light-induced chromatin compaction in Arabidopsis thaliana. PLoS Genet. 2009;5(9):e1000638.
71. Wang Y, Hu Q, Wu Z, Wang H, Han S, Jin Y, Zhou J, Zhang Z, Jiang J, Shen Y, et al. HISTONE DEACETYLASE 6 represses pathogen defence responses in Arabidopsis thaliana. Plant Cell Environ. 2017;40(12):2972–86.
72. Cigliano RA, Cremona G, Paparo R, Termolino P, Perrella G, Gutzat R, Consiglio MF, Conicella C. Histone deacetylase AtHDA7 is required for female gametophyte and embryo development in Arabidopsis. Plant physiology. 2013;163(1):431–40.
73. Zhao J, Li M, Gu D, Liu X, Zhang J, Wu K, Zhang X, Teixeira da Silva JA, Duan J. Involvement of rice histone deacetylase HDA705 in seed germination and in response to ABA and abiotic stresses. Biochem Biophys Res Commun. 2016;470(2):439–44.

74. Kim W, Latrasse D, Servet C, Zhou DX: **Arabidopsis histone deacetylase HDA9 regulates flowering time through repression of AGL19**. *Biochemical and biophysical research communications* 2013, **432**(2):394–398.
75. Kang MJ, Jin HS, Noh YS, Noh B. Repression of flowering under a noninductive photoperiod by the HDA9-AGL19-FT module in Arabidopsis. New Phytol. 2015;206(1):281–94.
76. van Zanten M, Zoll C, Wang Z, Philipp C, Carles A, Li Y, Kornet NG, Liu Y, Soppe WJ. HISTONE DEACETYLASE 9 represses seedling traits in Arabidopsis thaliana dry seeds. The Plant journal: for cell molecular biology. 2014;80(3):475–88.
77. Chen X, Lu L, Mayer KS, Scalf M, Qian S, Lomax A, Smith LM, Zhong X. **POWERDRESS interacts with HISTONE DEACETYLASE 9 to promote aging in Arabidopsis**. *eLife* 2016, 5.
78. Zheng Y, Ding Y, Sun X, Xie S, Wang D, Liu X, Su L, Wei W, Pan L, Zhou DX. Histone deacetylase HDA9 negatively regulates salt and drought stress responsiveness in Arabidopsis. J Exp Bot. 2016;67(6):1703–13.
79. Liu X, Chen CY, Wang KC, Luo M, Tai R, Yuan L, Zhao M, Yang S, Tian G, Cui Y, et al. PHYTOCHROME INTERACTING FACTOR3 associates with the histone deacetylase HDA15 in repression of chlorophyll biosynthesis and photosynthesis in etiolated Arabidopsis seedlings. Plant Cell. 2013;25(4):1258–73.
80. Gu D, Chen CY, Zhao M, Zhao L, Duan X, Duan J, Wu K, Liu X. Identification of HDA15-PIF1 as a key repression module directing the transcriptional network of seed germination in the dark. Nucleic acids research. 2017;45(12):7137–50.
81. Tang Y, Liu X, Liu X, Li Y, Wu K, Hou X. Arabidopsis NF-YCs Mediate the Light-Controlled Hypocotyl Elongation via Modulating Histone Acetylation. Molecular plant. 2017;10(2):260–73.
82. Luo M, Tai R, Yu CW, Yang S, Chen CY, Lin WD, Schmidt W, Wu K. Regulation of flowering time by the histone deacetylase HDA5 in Arabidopsis. The Plant journal: for cell molecular biology. 2015;82(6):925–36.
83. Liu C, Li LC, Chen WQ, Chen X, Xu ZH, Bai SN. HDA18 affects cell fate in Arabidopsis root epidermis via histone acetylation at four kinase genes. Plant Cell. 2013;25(1):257–69.
84. Bourque S, Jeandroz S, Grandperret V, Lehotai N, Aime S, Soltis DE, Miles NW, Melkonian M, Deyholos MK, Leebens-Mack JH, et al. The Evolution of HD2 Proteins in Green Plants. Trends in plant science. 2016;21(12):1008–16.
85. Wu K, Tian L, Zhou C, Brown D, Miki B. Repression of gene expression by Arabidopsis HD2 histone deacetylases. The Plant journal: for cell molecular biology. 2003;34(2):241–7.
86. Li H, Torres-Garcia J, Latrasse D, Benhamed M, Schilderink S, Zhou W, Kulikova O, Hirt H, Bisseling T. Plant-Specific Histone Deacetylases HDT1/2 Regulate GIBBERELLIN 2-OXIDASE2 Expression to Control Arabidopsis Root Meristem Cell Number. Plant Cell. 2017;29(9):2183–96.
87. Yano R, Takebayashi Y, Nambara E, Kamiya Y, Seo M. Combining association mapping and transcriptomics identify HD2B histone deacetylase as a genetic factor associated with seed dormancy in Arabidopsis thaliana. The Plant journal: for cell molecular biology. 2013;74(5):815–28.
88. Latrasse D, Jegu T, Li H, de Zelicourt A, Raynaud C, Legras S, Gust A, Samajova O, Veluchamy A, Rayapuram N, et al. MAPK-triggered chromatin reprogramming by histone deacetylase in plant innate immunity. Genome biology. 2017;18(1):131.
89. Luo M, Wang YY, Liu X, Yang S, Lu Q, Cui Y, Wu K. HD2C interacts with HDA6 and is involved in ABA and salt stress response in Arabidopsis. J Exp Bot. 2012;63(8):3297–306.
90. Zhao J, Zhang J, Zhang W, Wu K, Zheng F, Tian L, Liu X, Duan J. Expression and functional analysis of the plant-specific histone deacetylase HDT701 in rice. Frontiers in plant science. 2014;5:764.
91. Haigis MC, Guarente LP. Mammalian sirtuins–emerging roles in physiology, aging, and calorie restriction. Genes Dev. 2006;20(21):2913–21.
92. Liu X, Wei W, Zhu W, Su L, Xiong Z, Zhou M, Zheng Y, Zhou DX. Histone Deacetylase AtSRT1 Links Metabolic Flux and Stress Response in Arabidopsis. Molecular plant. 2017;10(12):1510–22.
93. Zhang F, Wang L, Ko EE, Shao K, Qiao H. Histone Deacetylases SRT1 and SRT2 Interact with ENAP1 to Mediate Ethylene-Induced Transcriptional Repression. Plant Cell. 2018;30(1):153–66.

94. Huang L, Sun Q, Qin F, Li C, Zhao Y, Zhou DX. Down-regulation of a SILENT INFORMATION REGULATOR2-related histone deacetylase gene, OsSRT1, induces DNA fragmentation and cell death in rice. Plant physiology. 2007;144(3):1508–19.
95. Zhang H, Zhao Y, Zhou DX. Rice NAD+-dependent histone deacetylase OsSRT1 represses glycolysis and regulates the moonlighting function of GAPDH as a transcriptional activator of glycolytic genes. Nucleic acids research. 2017;45(21):12241–55.
96. Lescot M, Dehais P, Thijs G, Marchal K, Moreau Y, Van de Peer Y, Rouze P, Rombauts S. PlantCARE, a database of plant cis-acting regulatory elements and a portal to tools for in silico analysis of promoter sequences. Nucleic acids research. 2002;30(1):325–7.
97. Zhang GQ, Liu KW, Li Z, Lohaus R, Hsiao YY, Niu SC, Wang JY, Lin YC, Xu Q, Chen LJ, et al. The Apostasia genome and the evolution of orchids. Nature. 2017;549(7672):379–83.
98. Wu ZG, Jiang W, Chen SL, Mantri N, Tao ZM, Jiang CX. Insights from the Cold Transcriptome and Metabolome of Dendrobium officinale: Global Reprogramming of Metabolic and Gene Regulation Networks during Cold Acclimation. Frontiers in plant science. 2016;7:1653.
99. Zou LH, Wan X, Deng H, Zheng BQ, Li BJ, Wang Y. RNA-seq transcriptomic profiling of crassulacean acid metabolism pathway in Dendrobium catenatum. Scientific data. 2018;5:180252.
100. Song XJ, Kuroha T, Ayano M, Furuta T, Nagai K, Komeda N, Segami S, Miura K, Ogawa D, Kamura T, et al. Rare allele of a previously unidentified histone H4 acetyltransferase enhances grain weight, yield, and plant biomass in rice. Proc Natl Acad Sci USA. 2015;112(1):76–81.
101. Nallamilli BR, Edelmann MJ, Zhong X, Tan F, Mujahid H, Zhang J, Nanduri B, Peng Z. Global analysis of lysine acetylation suggests the involvement of protein acetylation in diverse biological processes in rice (Oryza sativa). PloS one. 2014;9(2):e89283.
102. VanDrisse CM, Escalante-Semerena JC. Protein Acetylation in Bacteria. Annu Rev Microbiol. 2019;73:111–32.
103. Zhang J, Sprung R, Pei J, Tan X, Kim S, Zhu H, Liu CF, Grishin NV, Zhao Y. Lysine acetylation is a highly abundant and evolutionarily conserved modification in Escherichia coli. Molecular cellular proteomics: MCP. 2009;8(2):215–25.
104. Nakayasu ES, Burnet MC, Walukiewicz HE, Wilkins CS, Shukla AK, Brooks S, Plutz MJ, Lee BD, Schilling B, Wolfe AJ, et al: **Ancient Regulatory Role of Lysine Acetylation in Central Metabolism**. *mBio* 2017, 8(6).
105. Shi L, Tu BP. Acetyl-CoA and the regulation of metabolism: mechanisms and consequences. Curr Opin Cell Biol. 2015;33:125–31.
106. Chen C, Li C, Wang Y, Renaud J, Tian G, Kambhampati S, Saatian B, Nguyen V, Hannoufa A, Marsolais F, et al. Cytosolic acetyl-CoA promotes histone acetylation predominantly at H3K27 in Arabidopsis. Nature plants. 2017;3(10):814–24.
107. Shen Y, Wei W, Zhou DX. Histone Acetylation Enzymes Coordinate Metabolism and Gene Expression. Trends in plant science. 2015;20(10):614–21.
108. Earley KW, Shook MS, Brower-Toland B, Hicks L, Pikaard CS. In vitro specificities of Arabidopsis co-activator histone acetyltransferases: implications for histone hyperacetylation in gene activation. The Plant journal: for cell molecular biology. 2007;52(4):615–26.
109. Fong PM, Tian L, Chen ZJ. Arabidopsis thaliana histone deacetylase 1 (AtHD1) is localized in euchromatic regions and demonstrates histone deacetylase activity in vitro. Cell research. 2006;16(5):479–88.
110. Alinsug MV, Chen FF, Luo M, Tai R, Jiang L, Wu K. Subcellular localization of class II HDAs in Arabidopsis thaliana: nucleocytoplasmic shuttling of HDA15 is driven by light. PloS one. 2012;7(2):e30846.
111. Buszewicz D, Archacki R, Palusinski A, Kotlinski M, Fogtman A, Iwanicka-Nowicka R, Sosnowska K, Kucinski J, Pupel P, Oledzki J, et al. HD2C histone deacetylase and a SWI/SNF chromatin remodelling complex interact and both are involved in mediating the heat stress response in Arabidopsis. Plant Cell Environ. 2016;39(10):2108–22.
112. Krogan NT, Hogan K, Long JA. APETALA2 negatively regulates multiple floral organ identity genes in Arabidopsis by recruiting the co-repressor TOPLESS and the histone deacetylase HDA19. Development. 2012;139(22):4180–90.

113. Zhou Y, Tan B, Luo M, Li Y, Liu C, Chen C, Yu CW, Yang S, Dong S, Ruan J, et al. HISTONE DEACETYLASE19 interacts with HSL1 and participates in the repression of seed maturation genes in Arabidopsis seedlings. Plant Cell. 2013;25(1):134–48.
114. Wang L, Zhang F, Rode S, Chin KK, Ko EE, Kim J, Iyer VR, Qiao H. Ethylene induces combinatorial effects of histone H3 acetylation in gene expression in Arabidopsis. BMC Genomics. 2017;18(1):538.
115. Zhang F, Qi B, Wang L, Zhao B, Rode S, Riggan ND, Ecker JR, Qiao H. EIN2-dependent regulation of acetylation of histone H3K14 and non-canonical histone H3K23 in ethylene signalling. Nature communications. 2016;7:13018.
116. Zhang F, Wang L, Qi B, Zhao B, Ko EE, Riggan ND, Chin K, Qiao H. EIN2 mediates direct regulation of histone acetylation in the ethylene response. Proc Natl Acad Sci USA. 2017;114(38):10274–9.
117. Zhu Z, An F, Feng Y, Li P, Xue L, Jiang AM, Kim Z, To JM, Li TK. W et al: Derepression of ethylene-stabilized transcription factors (EIN3/EIL1) mediates jasmonate and ethylene signaling synergy in Arabidopsis. Proc Natl Acad Sci USA. 2011;108(30):12539–44.
118. Fang H, Liu X, Thorn G, Duan J, Tian L. Expression analysis of histone acetyltransferases in rice under drought stress. Biochem Biophys Res Commun. 2014;443(2):400–5.
119. Fu W, Wu K, Duan J. Sequence and expression analysis of histone deacetylases in rice. Biochem Biophys Res Commun. 2007;356(4):843–50.
120. Long JA, Ohno C, Smith ZR, Meyerowitz EM. TOPLESS regulates apical embryonic fate in Arabidopsis. Science. 2006;312(5779):1520–3.
121. Zhou C, Zhang L, Duan J, Miki B, Wu K. HISTONE DEACETYLASE19 is involved in jasmonic acid and ethylene signaling of pathogen response in Arabidopsis. Plant Cell. 2005;17(4):1196–204.
122. Choi SM, Song HR, Han SK, Han M, Kim CY, Park J, Lee YH, Jeon JS, Noh YS, Noh B. HDA19 is required for the repression of salicylic acid biosynthesis and salicylic acid-mediated defense responses in Arabidopsis. The Plant journal: for cell molecular biology. 2012;71(1):135–46.
123. Ding B, Bellizzi Mdel R, Ning Y, Meyers BC, Wang GL. HDT701, a histone H4 deacetylase, negatively regulates plant innate immunity by modulating histone H4 acetylation of defense-related genes in rice. Plant Cell. 2012;24(9):3783–94.
124. Chen QY, Chen DH, Shi Y, Si WS, Wu LS, Si JP. [Occurrence regularity of Dendrobium catenatum southern blight disease]. Zhongguo Zhong yao za zhi = Zhongguo zhongyao zazhi = China journal of Chinese materia medica. 2019;44(9):1789–92.
125. Kong L, Qiu X, Kang J, Wang Y, Chen H, Huang J, Qiu M, Zhao Y, Kong G, Ma Z, et al: **A Phytophthora Effector Manipulates Host Histone Acetylation and Reprograms Defense Gene Expression to Promote Infection**. *Current biology: CB* 2017, **27**(7):981–991.
126. Vijayapalani P, Hewezi T, Pontvianne F, Baum TJ. An Effector from the Cyst Nematode Heterodera schachtii Derepresses Host rRNA Genes by Altering Histone Acetylation. Plant Cell. 2018;30(11):2795–812.
127. Thompson JD, Higgins DG, Gibson TJ. CLUSTAL W: improving the sensitivity of progressive multiple sequence alignment through sequence weighting, position-specific gap penalties and weight matrix choice. Nucleic acids research. 1994;22(22):4673–80.
128. Tamura K, Stecher G, Peterson D, Filipski A, Kumar S: **MEGA6**: **Molecular Evolutionary Genetics Analysis version 6.0**. *Molecular biology and evolution* 2013, **30**(12):2725–2729.
129. Hu B, Jin J, Guo AY, Zhang H, Luo J, Gao G. GSDS 2.0: an upgraded gene feature visualization server. Bioinformatics. 2015;31(8):1296–7.
130. Matsuda S, Vert JP, Saigo H, Ueda N, Toh H, Akutsu T. A novel representation of protein sequences for prediction of subcellular location using support vector machines. Protein science: a publication of the Protein Society. 2005;14(11):2804–13.
131. Emanuelsson O, Brunak S, von Heijne G, Nielsen H. Locating proteins in the cell using TargetP, SignalP and related tools. Nature protocols. 2007;2(4):953–71.

132. la Cour T, Kiemer L, Molgaard A, Gupta R, Skriver K, Brunak S. Analysis and prediction of leucine-rich nuclear export signals. Protein engineering design selection: PEDS. 2004;17(6):527–36.
133. Chen C, Chen H, Zhang Y, Thomas HR, Frank MH, He Y, Xia R. TBtools: An Integrative Toolkit Developed for Interactive Analyses of Big Biological Data. Molecular plant. 2020;13(8):1194–202.
134. Kim D, Langmead B, Salzberg SL. HISAT: a fast spliced aligner with low memory requirements. Nature methods. 2015;12(4):357–60.
135. Pertea M, Pertea GM, Antonescu CM, Chang TC, Mendell JT, Salzberg SL. StringTie enables improved reconstruction of a transcriptome from RNA-seq reads. Nature biotechnology. 2015;33(3):290–5.

Tables

Table 1 Classification of DcHATs and DcHDACs

Gene classification	Gene name	Gene locus	UniProt accession	Exon number	CDS length (bp)	Protein length (AA)	Molecular weight	Isoelectric point
HAT superfamily								
CBP	DcHAC1a	LOC110095903	A0A2I0XAN9	18	5121	1706	192733.76	8.51
	DcHAC1b	LOC110100536	A0A2I0V8Y3	18	5160	1719	194331.75	8.42
GNAT	DcHAG1	LOC110114546	A0A2I0XBI2	12	1608	535	60057.06	5.27
	DcHAG2	LOC110098624	A0A2I0VU99	10	1395	464	52260.66	5.4
	DcHAG3	LOC110105870	A0A2I0WL22	9	1692	563	63415.9	8.79
MYST	DcHAM1*	LOC110108532	/	7	417	138	21971.89	8.29
	DcHAM2*	LOC110116247	A0A2I0VGJ4	4		234	26335.5	5.92
TAFII250	DcHAF1	LOC110113399	/	20	5460	1819	206088.58	5.83
HDACs superfamily								
RPD3/HDA1	DcHDA2a	LOC110109946	A0A2I0WRD3	10	1071	356	30616.14	6.25
	DcHDA2b*	LOC110115415	/	5	378	125	13714.7	4.62
	DcHDA5a	LOC110113261	A0A2I0VLY2	13	2058	685	76108.86	5.06
	DcHDA5b*	LOC110114271	A0A1J0CN47	3	499	165	18515.35	8.96
	DcHDA6	LOC110113780	A0A2I0W3W2	6	1500	499	55436.99	5.45
	DcHDA8	LOC110109348	A0A2I0VMQ1	8	1149	382	41545.88	5.44
	DcHDA9	LOC110103040	A0A2I0 × 9K5	14	1269	422	48473.71	5.05
	DcHDA14	LOC110111204	/	11	1335	444	48024.78	6.28
	DcHDA15	LOC110092582	A0A2I0VY14	17	1695	564	62307.71	6.31
	DcHDA19	LOC110097632	A0A2I0VJF9	7	1536	511	57896.33	5.3
SIR2	DcSRT1	LOC110114495	A0A2I0VLE6	14	1401	466	51980.46	9.09
	DcSRT2	LOC110097580	A0A2I0 × 263	11	1083	360	40173.94	9.18
HD2	DcHDT1	LOC110100482	A0A2I0 × 406	12	963	320	34978.36	4.8
	DcHDT2	LOC110103037	/	10	957	318	34112.37	4.86

* partial sequence.

Table 2 Predicted subcellular localization of DcHATs and DcHDACs.

Protein Name	SLP-LOCAL 1st /2nd candidate (RI)	TargetP (RC)	NetNES 1.1	Wolf PSORT	Uniprot
HAT family					
DcHAC1a	nucl_or_cyto/mito (2)	nucl_or_cyto (3)	1603-L	nucl: 13	Nucleus
DcHAC1b	mito/nucl_or_cyto (1)	mito (5)	1616-L	nucl: 12, vacu: 1	Nucleus
DcHAG1	nucl_or_cyto/chlo (1)	chlo (3)	/	chlo: 9, nucl: 3, mito: 2	/
DcHAG2	mitoc/nucl_or_cyto (1)	nucl_or_cyto (4)	107-L, 108-K, 109-L, 110-A,110-A	cyto: 9, nucl: 4	Nucleus
DcHAG3	nucl_or_cyto/chlo (1)	nucl_or_cyto (3)	410-L	cyto: 8, nucl: 2, mito: 2, chlo: 1	/
DcHAM1*	secr /mito (2)	secr (1)	21-I,24-L	cyto: 6.5, cyto_E.R.: 4, nucl: 3, plas: 2, mito: 1	/
DcHAM2*	nucl_or_cyto/secr (1)	nucl_or_cyto (3)	4-L,5-D,6-D,7-F,8-L,9-L,10-Q,11-L,13-M	/	/
DcHAF1	nucl_or_cyto/secr (6)	nucl_or_cyto (2)	1795-L	nucl: 7, cyto: 6	/
HDAC family					
DcHDA2a	chlo/mito (1)	nucl_or_cyto (5)	/	cyto: 8, nucl: 3, chlo: 1, vacu: 1	/
DcHDA2b*	nucl_or_cyto/secr (2)	nucl_or_cyto (2)	33-L,34-I,63-I	cyto: 5, extr: 4, nucl: 2, chlo: 1, plas: 1	/
DcHDA5a	nucl_or_cyto/mito (2)	nucl_or_cyto (3)	/	cyto: 9, nucl: 4	Nucleus
DcHDA5b*	mito/nucl_or_cyto (1)	nucl_or_cyto (4)	/	/	Nucleus
DcHDA6	chlo/mito (2)	nucl_or_cyto (5)	408-N,411-L	nucl: 10, chlo: 1, cyto: 1, mito: 1	Nucleus
DcHDA8	nucl_or_cyto/mito (1)	nucl_or_cyto (2)	/	cyto: 6, chlo: 3, nucl: 3, mito: 1	Nucleus
DcHDA9	nucl_or_cyto/mito (1)	nucl_or_cyto (2)	159-L	cyto: 7, nucl: 2, mito: 2, pero: 2	Nucleus
DcHDA14	secr /chlo (1)	chlo (5)	/	chlo: 8, cyto: 3, nucl: 2	/

RI: Reliability index ranges from 1 to 10. Higher RI value indicates more reliable predication.

RC: Reliability class from 1 to 5. The lower RC value indicates the safer the prediction. Secr: Secretory pathway.

The amino acid position and residue exhibiting predicted nuclear export signal (NES).

The numbers in parentheses indicate the prior probability that such protein localized to a given site is equal to the proportion of proteins in the data set. Abbreviations and the number of proteins of the localization site in the data set: nucl: nucleus (456); chlo: chloroplast (750); cyto: cytosol (432); E.R.: endoplasmic reticulum (69); cysk_nucl: cytoskeleton and nucleus (0); plas: plasma membrane (165); mito: mitochondria (210); cyto_nucl: cytosol and nucleus (11); pero: peroxisomes (52).

Subcellular locations predicted by Uniprot.

DcHDA15	nucl_or_cyto/secr (2)	nucl_or_cyto (2)	/	nucl: 4, cyto: 4, E.R.: 3, mito: 1, plas: 1	Nucleus
DcHDA19	nucl_or_cyto/mito (2)	nucl_or_cyto (1)	/	cyto: 6, nucl: 4, mito: 2, pero: 2	Nucleus
DcSRT1	nucl_or_cyto/secr (1)	nucl_or_cyto (2)	/	cyto: 6, nucl: 3, chlo: 2, mito: 1, plas: 1	/
DcSRT2	mito/chlo (2)	mito (4)	349-L,351-M,353-C,354-L,355-S,356-I	chlo: 10, mito: 3	Mitochondrion
DcHDT1	nucl_or_cyto/secr (3)	nucl_or_cyto (2)	/	nucl: 14	/
DcHDT2	nucl_or_cyto/secr (3)	nucl_or_cyto (2)	/	nucl: 14	/

RI: Reliability index ranges from 1 to 10. Higher RI value indicates more reliable predication.

RC: Reliability class from 1 to 5. The lower RC value indicates the safer the prediction. Secr: Secretory pathway.

The amino acid position and residue exhibiting predicted nuclear export signal (NES).

The numbers in parentheses indicate the prior probability that such protein localized to a given site is equal to the proportion of proteins in the data set. Abbreviations and the number of proteins of the localization site in the data set: nucl: nucleus (456); chlo: chloroplast (750); cyto: cytosol (432); E.R.: endoplasmic reticulum (69); cysk_nucl: cytoskeleton and nucleus (0); plas: plasma membrane (165); mito: mitochondria (210); cyto_nucl: cytosol and nucleus (11); pero: peroxisomes (52).

Subcellular locations predicted by Uniprot.

Figures

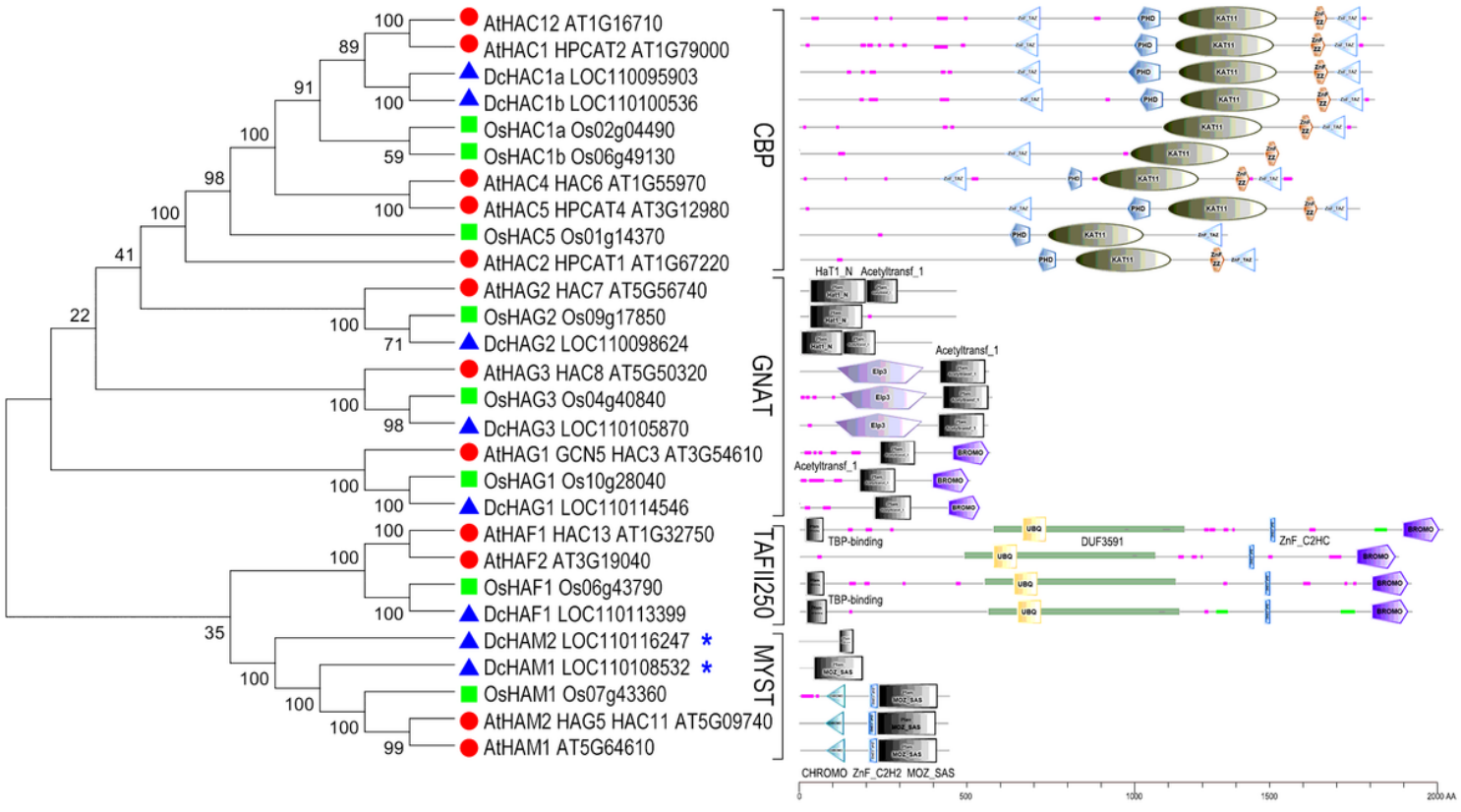

Figure 1

Phylogenetic analysis and domain organization of HATs in D. catenatum, compared with homologs in Arabidopsis and rice. Full-length HAT amino acid sequences from D. catenatum, Arabidopsis and rice were aligned via ClustalW, and the unrooted neighbor-joining (NJ) trees were constructed using MEGA7 software with the following settings: pairwise deletion option for gaps/missing data treatment; p-distance method for Substitution model; and Bootstrap test of 1000 replicates for internal branch reliability. Four families (CBP, GNAT, TAFII250, and MYST) are clustered here. The HAT proteins from D. catenatum, Arabidopsis and rice are indicated by green triangle, red circle and green square, respectively. Different conserved protein domains are colored as indicated.

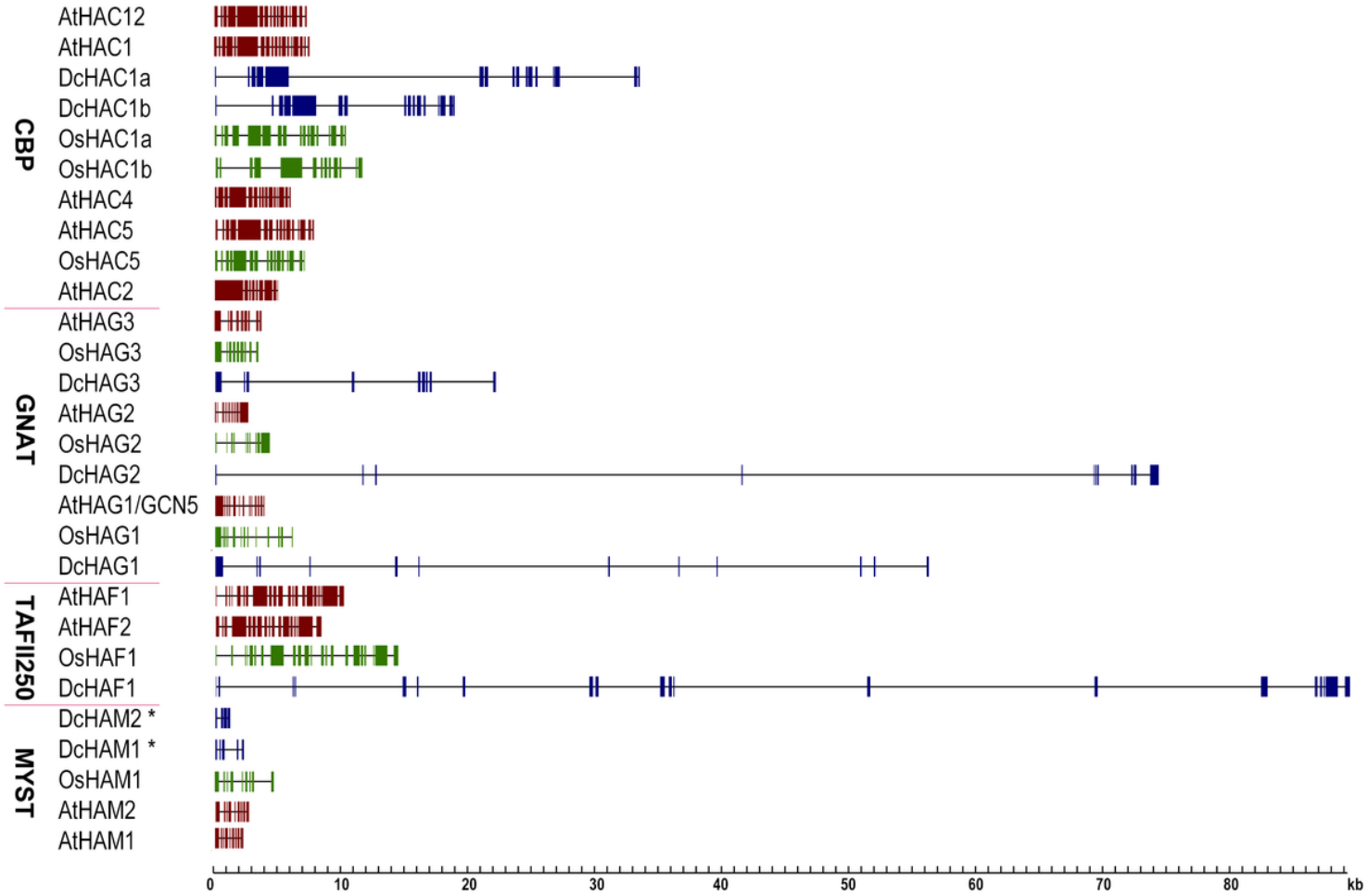

Figure 2

Gene structures of HAT family in D. catenatum, compared with homologs in Arabidopsis and rice. The solid boxes represent exons and black lines represent introns. Gene structures of HATs in D. catenatum, Arabidopsis and rice are indicated in blue, red, and green, respectively.

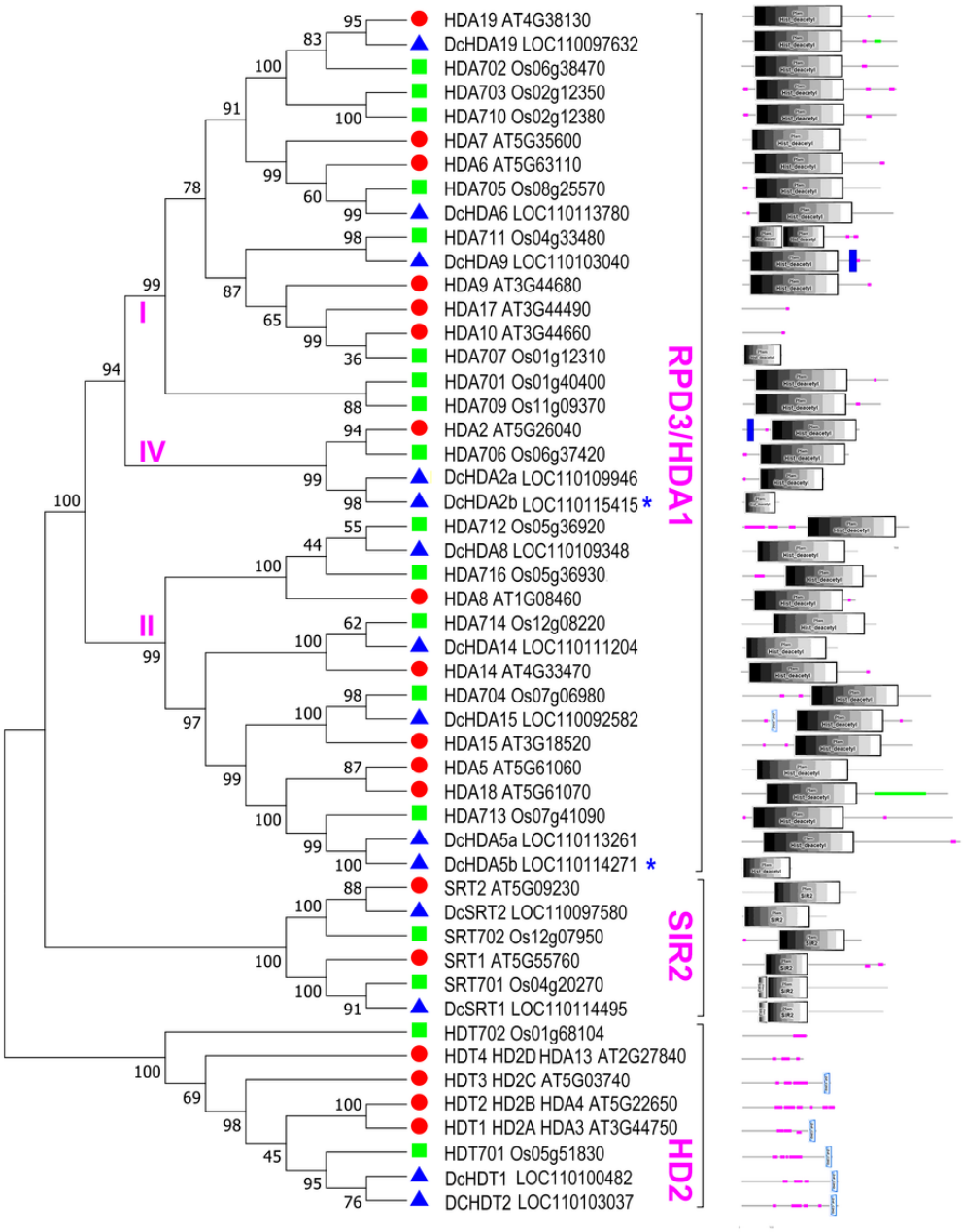

Figure 3

Phylogenetic analysis and domain organization of HDACs in D. catenatum, compared with homologs in Arabidopsis and rice. Full-length HDAC amino acid sequences from D. catenatum, Arabidopsis and rice were aligned via ClustalW, and the unrooted neighbor-joining (NJ) trees were constructed using MEGA7 software with the following settings: pairwise deletion option for gaps/missing data treatment; p-distance method for Substitution model; and Bootstrap test of 1000 replicates for internal branch reliability. HDAC family is divided into three families (RPD3/HDA1, SIR2, and HD2) here. The HDAC proteins from D. catenatum, Arabidopsis and rice are indicated by green triangle, red circle and green square, respectively. Different conserved protein domains are colored as indicated.

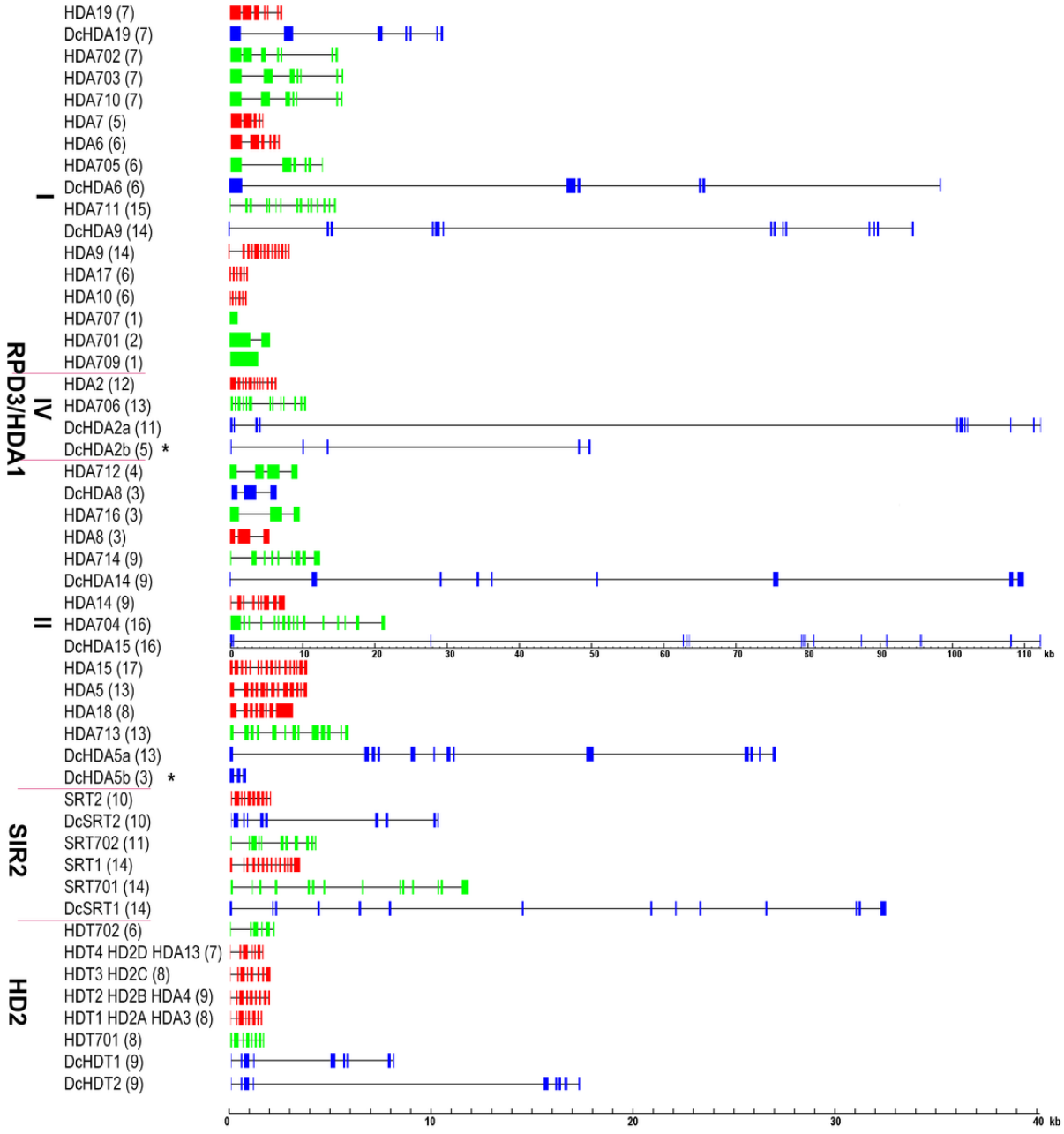

Figure 4

Gene structures of HDAC family in D. catenatum, compared with homologs in Arabidopsis and rice. The solid boxes represent exons and black lines represent introns. Gene structures of HDACs in D. catenatum, Arabidopsis and rice are indicated by blue red, and green, respectively.

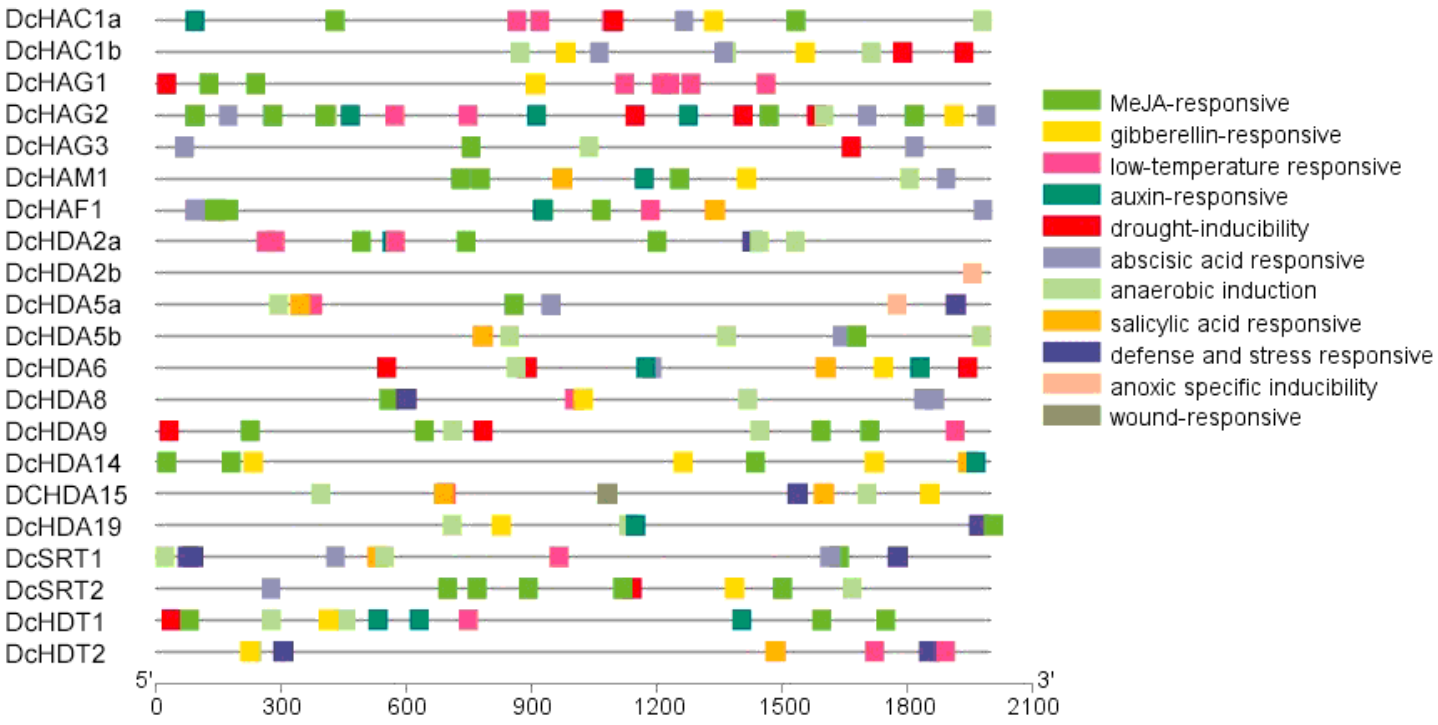

Figure 5

Prediction of cis-acting elements in DcHAT and DcHDAC gene promoter regions. Different color symbols indicate different cis-elements.

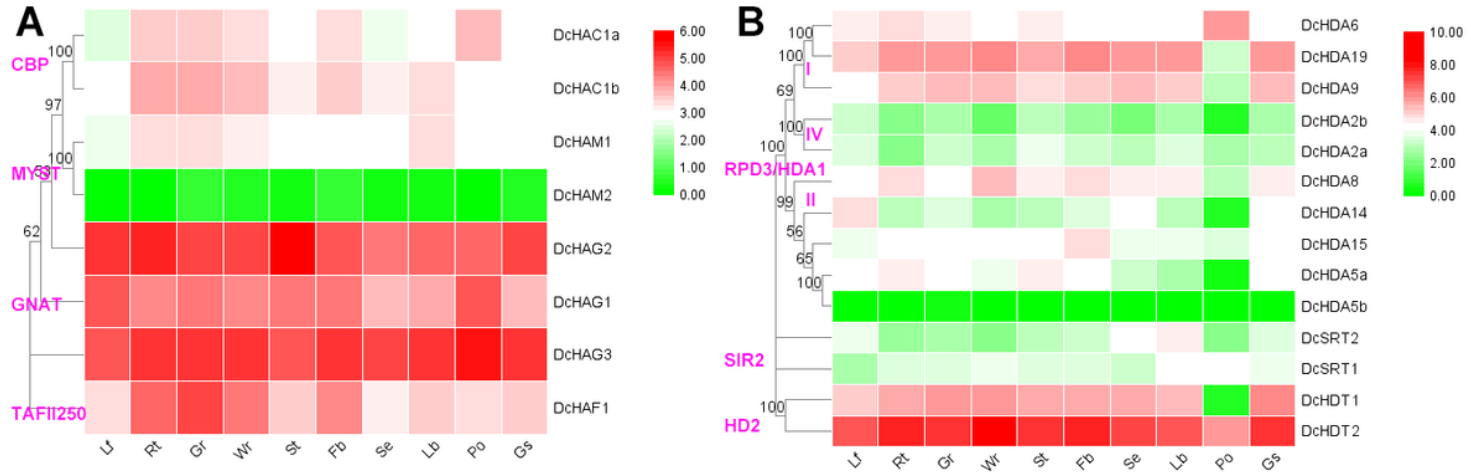

Figure 6

Tissue and organ expression profiles of DcHATs and DcHDACs. Heatmap was generated by TBtools software. Color scale represents log 2 of FPKM expression values, green and red indicate low and high level of gene expression, respectively. Lf: leaf, Rt: root, Gr: green root tip, Wr: white part of root, St: stem, Fb: flower bud, Se: sepal, Lb: labellum, Po: pollinia, and Gs: gynostemium.

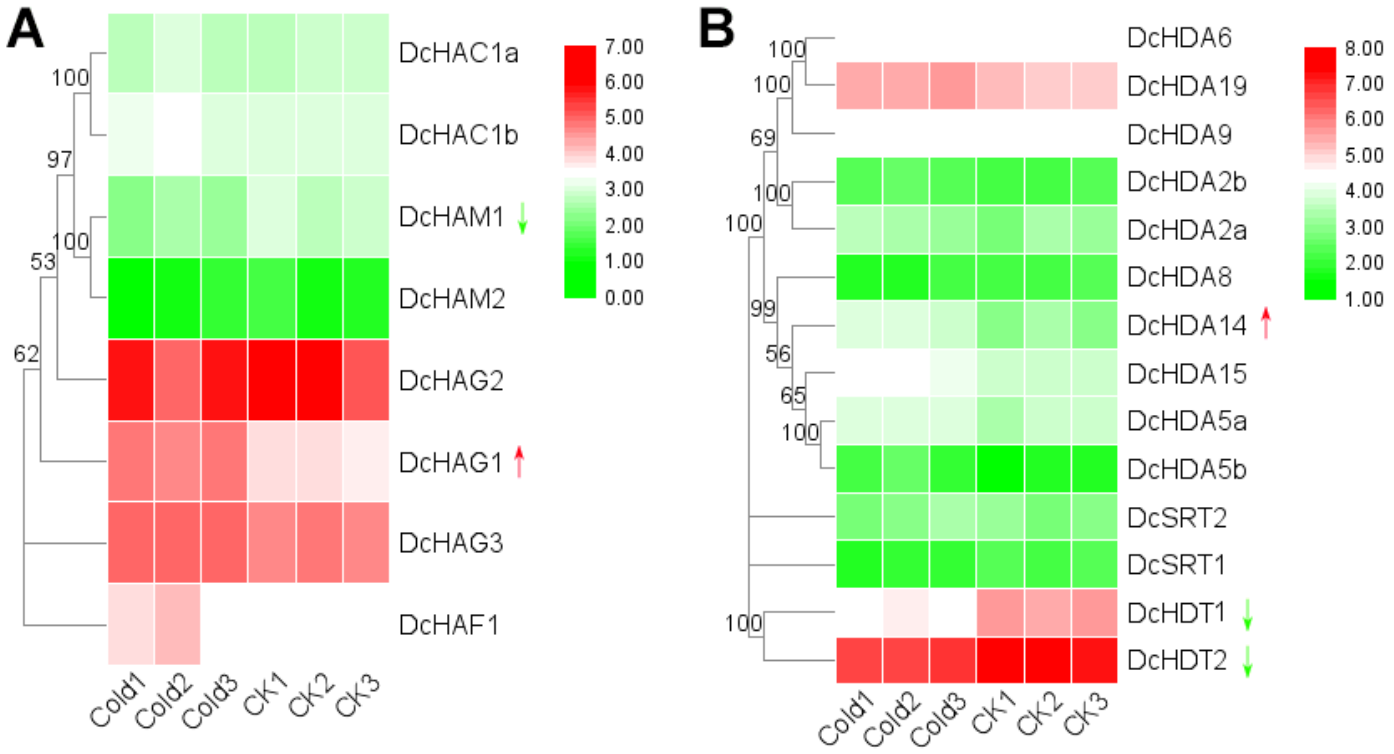

Figure 7

Expression of DcHATs and DcHDACs in response to cold stress. Heat map showing expression profiles of DcHAT/DcHDAC genes in leaves at 20 °C (control) and 0 °C (cold stress) for 20 h. Color scale from green end to red end indicating gene expression from low level to high level.

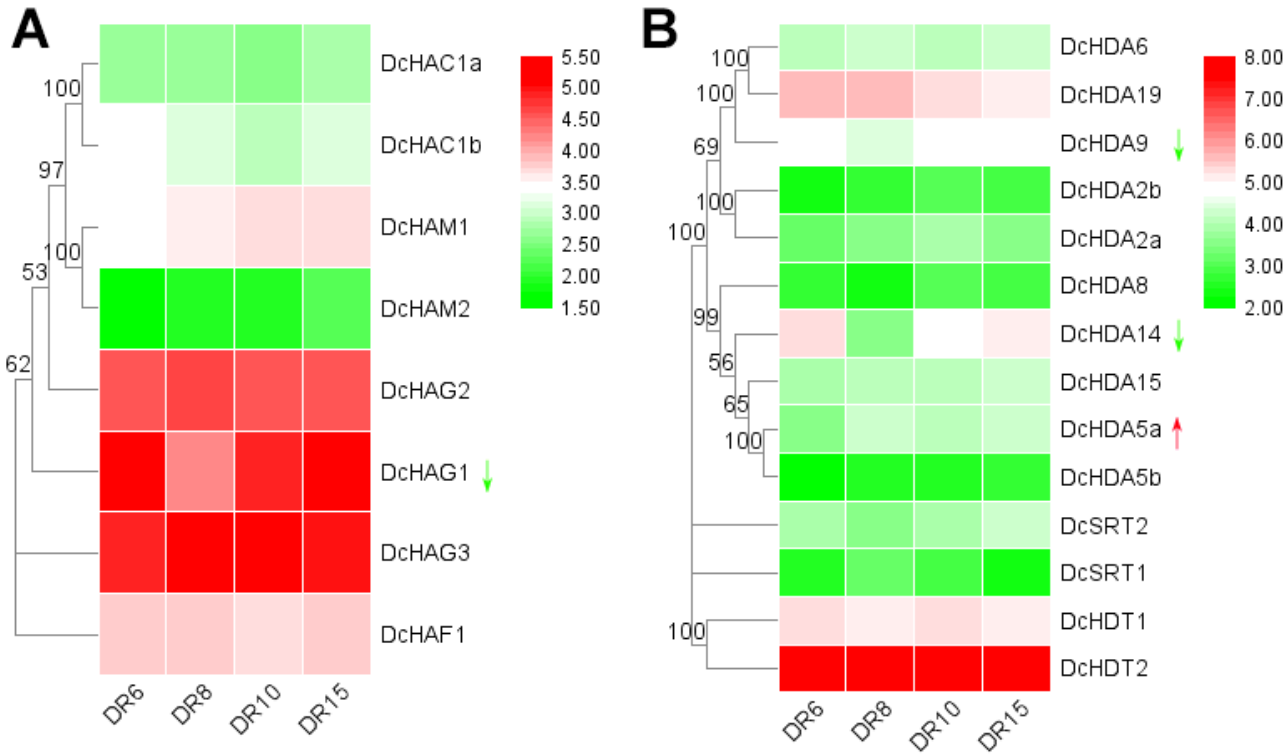

Figure 8

Expression of DcHATs and DcHDACs in response to drought stress. Heat map showing expression pattern of DcHATs and DcHDACs in leaves under different drought treatments. The seedlings were watered on the 1st day, dried from the 2nd to the 7th day, and re-watered on the 8th day. Leaves were harvested at different times; DR6, DR8, DR10, and DR15 indicate sampling at 18:30 on the 2nd, 7th, 8th, and 9th days, respectively. Color scale from green end to red end indicating gene expression from low level to high level.

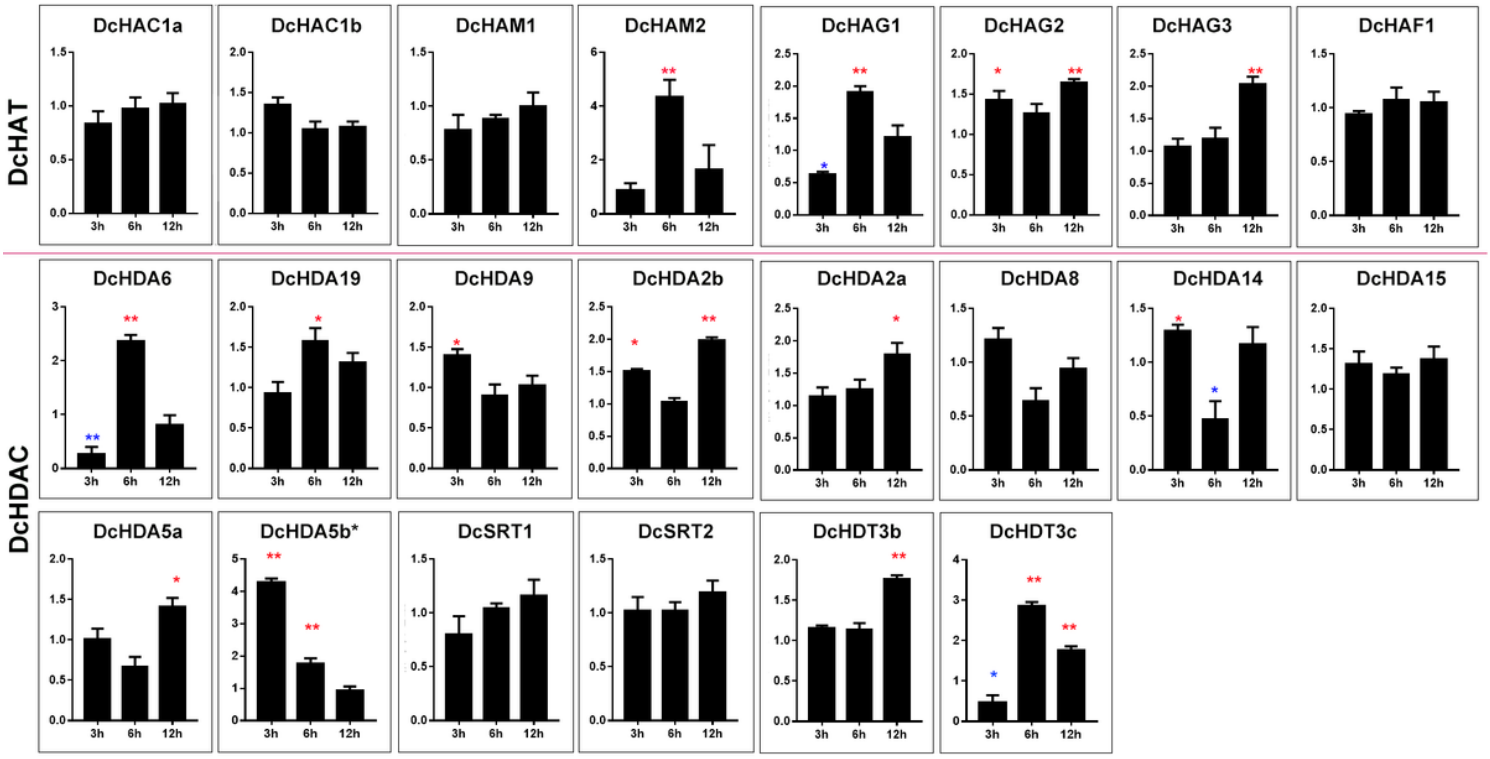

Figure 9

Expression of DcHATs and DcHDACs in response to heat shock. Expression profiles of DcHAT/DcHDAC genes in leaves at 20 °C (control) and 35 °C (heat shock) were detected by RT-qPCR. DcACTIN was used as an internal reference. Experiments were repeated three times. The error bars indicate SD and the asterisks indicate statistical significance between the heat shock (35°C) and the control (20°C) based on Student's t test (*, P<0.05; **, P<0.01).

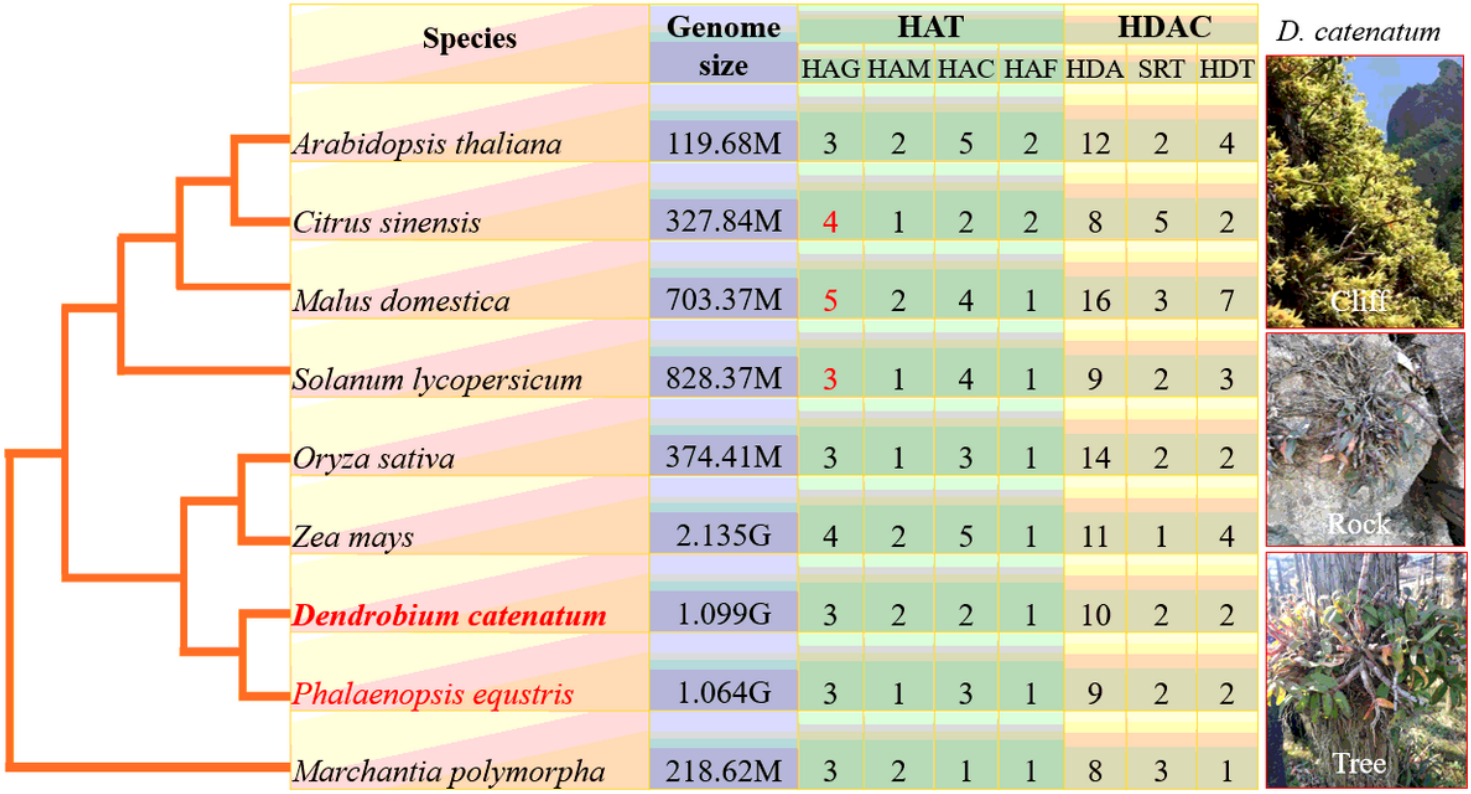

Figure 10

Distributions of HATs and HDACs in some representative species. Red digit in HAG column indicating the gene number have been modified based on more stringent screening criteria in this study. The photos on right showing D. catenatum grown on the cliff, artificial rock wall, and pine trunk, respectively.

Supplementary Files

This is a list of supplementary files associated with this preprint. Click to download.

- S6Primers.xlsx
- S5JAP1.tif
- S4drought.xlsx
- S3cold.xlsx
- S2organexpression.xlsx
- S1DcHATHDACseq.docx